2010

Control and Optimization of Laminar Incompressible Fluid Flow

David Anthony Brown

Control and Optimization of Laminar Incompressible Fluid Flow

(Thesis format: Integrated-Article)

by

David A. Brown

Graduate Program in Mechanical Engineering

A thesis submitted in partial fulfillment
of the requirements for the degree of
Master in Engineering Science

The School of Graduate and Postdoctoral Studies
The University of Western Ontario
London, Ontario, Canada

THE UNIVERSITY OF WESTERN ONTARIO
SCHOOL OF GRADUATE AND POSTDOCTORAL STUDIES

CERTIFICATE OF EXAMINATION

Supervisor	Examiners
Dr. Chao Zhang	Dr. Anthony Straatman
Co-Supervisor	Dr. Samuel Asokanthan
Dr. Jin Jiang	Dr. L. J. Brown

The thesis by

David Anthony Brown

entitled:

Control and Optimization of Laminar Incompressible Fluid Flow

is accepted in partial fulfillment of the
requirements for the degree of
Master in Engineering Science

Date_____

_____
Chair of the Thesis Examination Board

Abstract

The purpose of this thesis is to present a numerical algorithm for the dynamical optimization of fluid flow systems that contain both geometric and control variables. This problem was formulated in an optimal control setting by specifying some performance functional to be minimized subject to the constraints provided by the discretized state equations. An algorithm was presented and applied successfully in the feedforward case to a simple fluid flow problem. Linear quadratic feedback control of laminar incompressible fluid was also studied with the eventual intention of incorporating feedback control into the optimization process. A feedback law was developed numerically for incompressible fluid flow systems in some special cases, but after some numerical analysis it became clear that this method would have to be developed further before it could be of any practical use.

Keywords: Navier-Stokes equations; computational fluid dynamics; optimization; optimal control; quasi-Newton methods; feedback control; Riccati equations; linear quadratic regulator; perturbation methods.

Co-authorship Statement

The content of chapters 2,3, and 4 of this thesis have either been published, are in press, or are intended for future publication either in their current form or a modified form. All four papers were authored by the author of this thesis and were revised and approved by the author's supervisors, Dr. Chao Zhang and Dr. Jin Jiang, both of whom appear or will appear as co-authors on any publications.

Acknowledgements

I would like to thank my supervisors Dr. Chao Zhang and Dr. Jin Jiang who made this thesis possible through their support and feedback and for taking the time to review my work or provide guidance whenever it was needed. I would also like to thank my colleagues, especially Botao Peng and Rajeev Kumar, for many helpful discussions on CFD topics and for sharing their expert knowledge with me on more than one occasion.

Table of Contents

List of Figures

List of Tables

Nomenclature

A, B, C, E	State matrices
A_c	Cross-sectional area
A^s	Area of a control volume face
$\mathbf{A^s}$	Surface area vector normal to the surface
C_p	Heat capacity
D_p, D_s, D_t	Pressure, skin friction, and total drag
G^{*n}	Spatially discretized equation at the n^{th} time step
G	Spatially discretized terms of an equation at a time step
H	Hamiltonian
I	Identity matrix or integrand of the cost functional
J	Cost functional or performance index
L	Lagrangian
M	Linear map
M_p	Mass
N, Q, R	Weighting matrices
N	Number of time steps
P	Riccati solution matrix
Re	Reynolds number
S, W	Linear spaces
S	Surface
S_v	Matrix whose columns are an orthonormal basis for S
T	Temperature
$\bar{\mathbf{V}}$	Lagged velocity vector
$\forall$	Volume
$\mathbf{W}$	Fully discretized system parameters
$\mathbf{X}$	Fully discretized state
$\mathbf{Y}$	Fully discretized control parameters
$\mathbf{Z}$	Fully discretized geometric parameters
a, b, c	Active coefficients
$\mathbf{b}$	Vector
d	Number of spatial dimensions
f	Continuous real-valued system
h	Convective heat transfer coefficient
i, j	Indices

k	Thermal conductivity
$\mathbf{k}$	Constant vector
l	Width of the flow field
m	$d \cdot n$
n	Number of computational nodes
$\hat{\mathbf{n}}$	Unit vector normal to a surface
$\mathbf{p}$	Pressure vector (dependent variable)
q	Heat
r_1, r_2	Radii of the ellipse
$\hat{r}$	Unit vector normal to the surface
s	Basis vector for S or S^c
t	Time (independent variable)
$\mathbf{u}$	Control vector
$\mathbf{v}$	Velocity vector (dependent variable)
$\mathbf{w}$	Vector
$\mathbf{x}$	State vector
α, β, γ	Real-valued constants
δ	Perturbation or variation, or in some cases the boundary operator
ε	Small positive real number
μ	Viscosity
ρ	Density
ξ, η	Spatial coordinates
$\boldsymbol{\psi}$	Lagrangian multiplier vector
σ	Stefan-Boltzmann constant
Γ	Subset of Ω
Ω	Computational domain

Operators

$\Delta(\cdot)$	Difference
$\nabla(\cdot)$	Gradient operator
$\nabla \cdot (\cdot)$	Divergence operator
$\nabla^2(\cdot)$	Laplacian operator

Subscripts

E, W, P	East node, West node, and Principal node
O	Of the previous time step
f	Final
nb	Neighbouring node
r	Randomly generated
ξ	In the ξ direction
0	Of the perturbed system

Superscripts

T	Matrix or vector transpose
eq	Equilibrium
c	Orthogonal complement
n	Index
ss	Solution at steady state
$*$	Particular solution
$\#$	Minimum norm solution

Chapter 1

Introduction and Related Literature

This thesis is produced in integrated article format containing three articles. Since each of these articles contains an independent introduction this section will be brief and will contain a rather broad overview of the material, some insight into the objectives of this thesis, and of course a review of the most relevant literature publications.

1.1 Background and Thesis Direction

Enhancing the performance of existing design systems is currently an important engineering topic. In the automotive or aerospace industry, for example, improving engine performance or reducing drag can result in lower fuel consumption, which will effectively reduce the operating cost and reduce the emission of pollutants. With advances in numerical modeling practices and computer technology, the practicality of numerical algorithms for the optimization of even the most complex dynamical systems has become increasingly realistic. Performance enhancement can be obtained either by the application of a control variable or by changing the geometry of the system itself. In either case, the ability to construct an accurate numerical model for the system in question can be of great assistance in improving the system design. However, for complex dynamical systems such as most realistic fluid flow or heat transfer systems, exhaustively running simulations for varying combinations of parameters may be unreasonable from a computational perspective, since running even one simulation may take many hours. Moreover, by using some more advanced techniques we can improve the system performance more than we ever could by basic "guess and check" methods, and with far less computational cost.

The ultimate goal of this thesis is to develop and test a general numerical algorithm for the performance optimization of fluid flow systems containing a combination of geometric and control variables and also to develop a feedback control law for an optimized system. This problem is formulated mathematically as the minimization of some performance index (or cost functional) subject to the state equations, which are treated as dynamical constraints.

The general problem of minimizing a function over several variable system parameters subject to constraints is well established. This problem can be solved numerically by evaluating the performance index and its gradient at a point, then minimizing according to any well-established minimization algorithm, such as Newton's method or the conjugate gradient method. However, evaluation of the gradient of the performance index by the most obvious methods (finite differences, for example) requires multiple simulations of the system at each iterative step and the computational time required will become unfeasible when the number of system parameters is high. For this reason, the well-established discrete adjoint method is used to compute the gradient at each iterative step. This will result in less computational time required at each iterative step so that the total computational time at each step is less than double the computational cost of a full system simulation. Unavoidably, the data storage requirement will be high for any numerical optimization algorithm since it is not possible to optimize the system without considering all system data at each iterative step. This is especially problematic for control of unsteady systems since data will have to be stored for all time steps.

The contribution to this subject from this thesis is the coupling of geometric and control optimization using the discrete adjoint method to improve the performance of the system beyond either individual optimization process. Since the primary interest has been the development of the algorithm the formulation was presented in the most general case, assuming as little as possible about the form of the control or geometric variables and assuming that the problem is unsteady since the steady

problem is merely a special case of the unsteady problem.

Though the mathematical formulation of the problem is very self sufficient it is important to investigate the functionality of this algorithm to identify any potential problems with its application that may affect its use. When the system dynamics are subject to multiple design variables the cost functional may exhibit several minima or saddle points, which can cause slow convergence or convergence to a point which is not a global minimum. Since the computational cost is already large, it is important to have some insight into this problem so that convergence problems can be avoided. Some simulations are performed on a simple two-dimensional sample problem to identify such problems and propose measures to avoid these difficulties.

The literature on control and geometry optimization is far more extensive than in the area of feedback control for fluid flow systems. This can mainly be attributed to the impracticality of feedback law implementation due to difficulties in data acquisition, the mathematical complexity of developing the feedback laws, and numerical limitations in solving the nonlinear equations that result. With improvements in technology such as MEMS and advances in computer technology, feedback control for fluid flow systems is becoming less impractical and there has been more interest in the mathematical treatment of this problem.

The approach to feedback flow control taken in this thesis is to discretize the Navier-Stokes equations spatially, resulting in a coupled system of first and zeroth order time differential equations. In general such discretization processes for both fluid flow and heat transfer systems result in a linearized system with the property of highly non-normal (nearly parallel) eigenvectors. Such systems typically exhibit high transient energy growth. Though it is possible to control such systems by standard methods such as PID or pole placement, these methods rely on eigenvalue information which does not reflect eigenvector information and hence this system property is ignored. Ignoring this property can result in eratic behaviour such as high overshoot or heavy oscillations. Rather, it is preferable to use a method that either accounts

for eigenvector properties or penalizes the control input directly, such as optimal control. Especially popular are the special optimal control methods of H^∞ control or H^2 control, the latter of which will be analyzed in this thesis.

In this thesis the derivation for a linear feedback law for incompressible laminar fluid flow is presented according to the same performance criteria specified for the open loop case. Due to the unusual form that the discretized Navier-Stokes equations take (differential equations coupled with algebraic equations) the derivation had to be approached from first principles directly from variational calculus. The state-costate system was developed in the most general case but could only be reduced to a matrix algebraic Riccati system in some special cases. Despite this minor success, the equations resulting were nonlinear matrix algebraic equations which could not be solved numerically. Therefore an alternate method was investigated and the system Riccati equation was used to numerically test the results.

1.2 Summary of the Articles Contained in this Thesis

There are three articless contained in this thesis, each assigned an individual chapter number. Two of these have been published in conference proceedings, one is in press, and at least one will be submitted for journal publication as well. All articles have been modified from their original version to meet the formatting requirements of this thesis.

The paper herein denoted *Chapter 2* has been submitted to the *18th Annual Conference of the CFD Society of Canada* and is entitled *Performance Optimization for Fluid Flow Systems with Variable Geometric and Control Parameters* and will also be submitted to the journal *Optimization and Engineering.* This paper presents the mathematical formulation and accompanying algorithm for the application of a dy-

namical optimization procedure for fluid flow or heat transfer systems that contain some combination of geometric and control variables. The discrete adjoint method is used to obtain the gradient information needed for the application of a minimization process with reasonable computational and storage requirements. The algorithm is validated on a simple two dimensional fluid flow system and some observations are made regarding the convergence, accuracy, and reliability of the algorithm.

The article denoted *Chapter 3* is entitled *Feedback control of heat transfer systems by the numerical method of lines* and has been published in the proceedings of *The 2009 ASME Summer Heat Transfer Conference.* In this paper, an optimal feedback law was applied from first principles to a simple one dimensional nonlinear heat transfer system using a spacial discretization and solving the resulting system of ordinary differential equations. The purpose of this exercise was to investigate the effectiveness of applying a feedback law to a numerically simulated nonlinear dynamical system by this partial discretization method. This paper also includes simulation about an evolving linearization point, which was too complex to perform for the Navier-Stokes equations.

The article denoted *Chapter 4* is entitled *Feedback control of fluid flow systems using a finite volume discretization.* This article has not been submitted for publication but incorporates some of the results form our paper *Optimal feedback control of the Navier-Stokes equations*, published in *The 20th International Symposium on Transport Phenomenon.* This article details the mathematical formulation for feedback control of the Navier-Stokes equations using linear quadratic regulation. A numerical method is presented for the generation of a feedback law and its validity is investigated by some numerical analysis as well as direct simulation. This chapter is in the preparation to be submitted to the journal *International Journal for Numerical Methods in Fluids.*

1.3 Literature Review

As mentioned, the background material relating to Chapter 2 is well-established. Here we use a discrete adjoint method applied directly to the discretized Navier-Stokes equations to develop an equation for the gradient of a specified performance index with relatively low computational cost. Early publications on the use of the discrete adjoint method for performance optimization of fluid flow systems include Reuther and Jameson (1994) and Korivi et al (1992). The first of these details the discrete adjoint method in terms of an airfoil design problem for steady operating conditions and provides a numerical problem for validation. The second investigates numerical methods for solving the adjoint equations, including some detailed analysis of the advantages of certain numerical solution methods. For a thorough treatment of the subject of discrete adjoint methods and optimal desing problems we primarily referred to Haslinger and Mäkinen (2003) and Laporte and Tallec (1999). In Rumpfkeil and Zingg (2008), the authors presented the formulation for the discrete adjoint method applied to time-variant systems. This article also presented two numerical examples, one of which was a control problem with a time-periodic control law and the second of which was a geometric optimization problem. The subject of Chapter 2 is a direct extension of this work to systems with mixed parameter types. The text Nocedal and Wright (2006) details several optimization schemes relevant to this paper, including quasi-Newton and gradient methods.

Feedback control of fluid flow systems has been approached by many diverse angles and to our knowledge there is no complete textbook on the subject. The textbook chapter Gad-el-Hak and Bewley (2006) does however provide a recent review of current progress in this field. One of several major obstacles in the solution to the linear control generation from the discretized Navier-Stokes equations is that the discretization takes on a degenerate form, as we will see. A number of strategies have been used to approach this problem. An investigation of the existence and uniqueness of such a control is given by Cobb (1983). One approach to solving the degenerate control

problem is model reduction. A mathematical formulation for the specific form of the degenerate control problem as encountered in fluid mechanics is presented in Hechme et al (2008). In Rediniotis et al (2002) the authors use a model reduction method based on a correlation matrix from either a physical or numerical experiment to acquire a feedback law. Since the finite volume discretization was not easily amenable to the method of Hechme et al (2008) we chose instead to use a perturbation technique similar to what has been done in Stoyanov (2006), in which the author developed a feedback law for the finite-element discretized Stokes equations.

The solution to the linear quadratic regulator problem by any method requires the solution to a nonlinear matrix algebraic Riccati equation, the matrices involved being quite large, creating a formidable numerical challenge in all but the simplest of cases and resistant to numerical solutions by established numerical algorithms. Some recent algorithms have been developed for this equation tuned to address certain problems encountered in fluid flow control, including Penzl (1999) and Borggaard et al (2004).

The subject of optimal control is well-established and thoroughly studied, especially for the special case of linear quadratic regulation which is particularly emphasized in this thesis. Some important control texts which we referred to are Bryson and Ho (1969); Brocket (1969); Lee and Markus (1967). We also referred to Pinch (1993) for a comprehensive derivation of the Euler-Lagrange equations.

Since the numerical procedures developed in this thesis were highly interactive with the state equations we chose to hard code in Matlab the dynamical systems that we analyzed rather than use any computational software for fluid mechanics. Though this proved rather time consuming it was easier to produce and debug the control-related matrices when they were generated directly from the active coefficients of the discretized system. For the basic principles of fluid mechanics we referred primarily to Patankar (1980). A change of coordinates approach was taken to deal with the non-orthogonal mesh for the channel flow around an ellipse, for which we referred to both Thompson et al (1985) and Liseikin (1999) for the methodology.

1.4 References

Borggaard J, Burns J, Zietsman L (2004) Computational challenges in control of partial differential equations. In: 2nd AIAA Flow Control Conference

Brocket RW (1969) Finite Dimensional Linear Systems. John Wiley & Sons, Inc.

Bryson AE, Ho YC (1969) Applied Optimal Control. Blaisdell Publishing Company

Cobb D (1983) Descriptor variable systems and optimal state regulation. IEEE Transactions on Automatic Control 28:601–611

Gad-el-Hak M, Bewley TR (2006) MEMS: Introduction and Fundamentals, CRC Press, chap 15

Haslinger J, Mäkinen RAE (2003) Introduction to Shape Optimization. SIAM

Hechme G, Nechepurenko YM, Sadkane M (2008) Model reduction for a class of linear descriptor systems. Journal of Computational and Applied Mathematics 229:54–60

Korivi VM, Taylor III AC, Newman PA, Hou GW, Jones HE (1992) An incremental strategy for calculating consistent discrete sensitivity derivatives. Tech. Rep. NASA TM 104207, NASA Langley Research Center, Hampton,VA

Laporte E, Tallec PL (1999) Numerical Methods in Sensitivity Analysis and Shape Optimization. Springer

Lee EB, Markus L (1967) Foundations of Optimal Control Theory. J. Wiley and Sons

Liseikin VV (1999) Grid Generation Methods. Springer

Nocedal J, Wright SJ (2006) Numerical Optimization, Second Edition. Springer

Patankar SV (1980) Numerical Heat Transfer and Fluid Flow. Hemisphere Publishing Corporation

Penzl T (1999) LyaPack Users' Guide (Version 1.0). Available at http://www.netlib.org/lyapack/guide.pdf

Pinch ER (1993) Optimal Control and the Calculus of Variations. Oxford University Press Inc.

Rediniotis OK, Ko J, Kurdila AJ (2002) Reduced order nonlinear Navier-Stokes models for synthetic jets. Journal of Fluids Engineering 124:433–443

Reuther J, Jameson A (1994) Control theory based airfoil design for potential flow and a finite volume discretization. In: 32nd Aerospace Sciences Meeting and Exhibit, Reno,NV, AIAA-94-0499

Rumpfkeil MP, Zingg DW (2008) The optimal control of unsteady flows with a discrete adjoint method. Optimization and Engineering

Stoyanov MK (2006) Optimal linear feedback controller for incompressible fluid flow. Master's thesis, Virginia Polytechnic Institute and State University

Thompson JF, Warsi ZUA, Mastin CW (1985) Numerical Grid Generation: Foundation and Applications. Elsevier Science Publishing Co., Inc.

Chapter 2

Performance Optimization for Fluid Flow Systems with Variable Geometric and Control Parameters

2.1 Introduction

Numerical optimization methods have played an increasingly important role in shape and control optimization for complex dynamical systems. This is especially true for dynamical systems that are governed by nonlinear partial differential equations, such as most realistic fluid flow systems. The effective use of such methods is made possible by the increasing availability of high-performance computational tools and significant developments in computational fluid dynamics over recent decades. Numerical methods are not reliable enough to produce ideal system design without physical experimentation to verify the results. However, they can help considerably to guide the initial design process or suggest improvements on an existing design before any expensive experiments are conducted.

Design optimization can be formulated mathematically as minimizing some performance index (or cost function) subject to the governing state equations, which are treated as constraints. Many numerical methods exist for the solution of problems described as such by using the information from the evaluation of the function at one point to determine a "better" point until the minimum is reached. Some relevant examples include the gradient method or Newton's method (Nocedal and Wright, 2006), both of which require for the gradient to be calculated at each iterative step. For numerically modeled fluid flow systems, computing the gradient by standard finite difference techniques will generally require several full simulations of the system at each iterative step. Though it is possible to optimize the system in this fashion, one simulation of the system is often very computationally expensive and so a control theory-based discrete adjoint method will be used to compute the gradient in this study. Such methods are well established for both control and geometry optimization. Early works on the subject include Reuther and Jameson (1994) and Korivi et al (1992). A thorough treatment of the subject can be found in Laporte and Tallec (1999) or Haslinger and Mäkinen (2003). Recently, Rumpfkeil and Zingg (2008) developed the discrete adjoint method for transient fluid flow systems and applied it successfully to two fluid flow optimization problems. The purpose of the current study is to extend this process

to systems containing both geometric and control variables.

The objective of the current study is to couple geometry and control optimization procedures to globally optimize the performance of a dynamical system. The mathematical formulation of the problem is presented in a general framework and a numerical experiment is conducted for drag minimization of two-dimensional channel flow around an elliptical obstruction. The flow dynamics are governed by the Navier-Stokes equations which were discretized according to the finite volume method of Patankar (1980). The computational mesh for the numerical experiment is non-orthogonal and a coordinate transformation is used to solve the state equations (Thompson et al, 1985; Liseikin, 1999). A thorough treatment of numerical optimization techniques, especially quasi-Newton methods, can be found in Nocedal and Wright (2006).

2.2 Formulation

Define a dynamical system with governing equations $\mathbf{S}$ on a finite domain Ω and over a finite time interval $[0, t_f]$. The system contains several geometric design parameters $\mathbf{Z}$ which are not a function of time or space. In the case where the objective is the optimal shape for a system boundary, the simplest formulation of the problem is to treat the boundary as a series of stationary points in the computational domain. This formulation allows for the problem to be treated as an optimization problem over several spatial parameters where the spacial dependence is not explicit. The system also contains several control parameters $\mathbf{Y}$ which are treated as being independent of space and time. In the case where each control variable has the form $Y_i = Y_i(t)$, the parameter is made independent of time by discretizing and treating it as several parameters $Y_i(t) \rightarrow Y_i^n$, $n = 1 \ldots N$, where N is the number of time steps. We may also have $Y_i(t) = g(\mathbf{Y}_i^c, t)$, where $g(t)$ is pre-determined up to the constant parameters $\mathbf{Y}_i^c$, which may be vectors.

2.2.1 The General Case

For ease of notation, introduce $\mathbf{W} = [\mathbf{Y}^T, \mathbf{Z}^T]^T$. To quantify the performance of the system we introduce the quantity J, referred to as the cost function or performance index, along

with its discretization over N time steps:

$$J = \int_0^{t_f} I(\mathbf{X}(t), \mathbf{W}(t))\, dt \to \sum_{n=1}^{N} I^n\left(\mathbf{X}^n, \mathbf{W}\right). \tag{2.1}$$

The dynamical system for optimization will be governed by a (system of) nonlinear partial differential equation(s). The spatial discretization of this (system of) equation(s) at the n^{th} time step will be denoted G^{*n}. The transient term is assumed to be first order and linear (which is generally the case in fluid flow and heat transfer problems) and can be discretized by any number of accepted discretization procedures. Using first order implicit time discretization, the equations will take the form:

$$G^{*n}\left(\mathbf{X}^n, \mathbf{X}^{n-1}, \mathbf{W}\right) = \frac{d\mathbf{X}^n}{dt} + G\left(\mathbf{X}^n, \mathbf{W}\right) \to \frac{\mathbf{X}^n - \mathbf{X}^{n-1}}{\Delta t} + G\left(\mathbf{X}^n, \mathbf{W}^n\right) = 0. \tag{2.2}$$

The derivation for the discrete adjoint derivative will assume this discretization. The effects of assuming some other time discretizations are demonstrated by Rumpfkeil and Zingg (2008).

We wish to minimize (2.1) subject to the constraints (2.2). This problem can be solved by applying a minimization algorithm to J. To do this we will need to compute the gradient ∇J by the discrete adjoint method. We define the Lagrangian of the system by appending the state equations to the cost function:

$$L = \sum_{n=1}^{N} \left[I^n\left(\mathbf{X}^n, \mathbf{W}\right) + \left(\boldsymbol{\psi}^n\right)^T G^{*n}\left(\mathbf{X}^n, \mathbf{X}^{n-1}, \mathbf{W}\right) \right] \tag{2.3}$$

using the Lagrangian multiplier functions $\boldsymbol{\psi}^n$. We proceed now to set the gradient $\nabla L = [\nabla_{\boldsymbol{\psi}} L\ \nabla_{\mathbf{X}} L\ \nabla_{\mathbf{W}} L] = 0$. The quantity $\nabla_{\boldsymbol{\psi}} L = 0$ produces the state equations which are

automatically satisfied. The quantity $\nabla_{\mathbf{X}} L$ is expanded to show its internal structure:

$$
\begin{aligned}
(\nabla_{\mathbf{X}} L)^T = & \\
& \begin{pmatrix}
(\nabla_{\mathbf{X}^1} G^{*1})^T & (\nabla_{\mathbf{X}^1} G^{*2})^T & 0 & \cdots & 0 \\
0 & (\nabla_{\mathbf{X}^2} G^{*2})^T & (\nabla_{\mathbf{X}^2} G^{*3})^T & \cdots & 0 \\
\vdots & \vdots & \vdots & \vdots & \vdots \\
0 & 0 & 0 & \cdots & (\nabla_{\mathbf{X}^{N-1}} G^{*N})^T \\
0 & 0 & 0 & \cdots & (\nabla_{\mathbf{X}^N} G^{*N})^T
\end{pmatrix}
\begin{pmatrix}
\boldsymbol{\psi}^1 \\ \boldsymbol{\psi}^2 \\ \vdots \\ \boldsymbol{\psi}^{N-1} \\ \boldsymbol{\psi}^N
\end{pmatrix} \\
& + \begin{pmatrix}
(\nabla_{\mathbf{X}^1} I^1)^T \\
(\nabla_{\mathbf{X}^2} I^2)^T \\
\vdots \\
(\nabla_{\mathbf{X}^{N-1}} I^{N-1})^T \\
(\nabla_{\mathbf{X}^N} I^N)^T
\end{pmatrix} = \mathbf{0}. \quad (2.4)
\end{aligned}
$$

Though the system is coupled we recognize that the lower block is decoupleable from the rest of the system. Hence we can solve the following equation independently:

$$\boldsymbol{\psi}^N = -\left(\left(\nabla_{\mathbf{X}^N} G^{*N} \right)^{-1} \right)^T \nabla_{\mathbf{X}^N} I^N. \quad (2.5)$$

The rest of the system can be solved recursively according to:

$$\boldsymbol{\psi}^n = -\left((\nabla_{\mathbf{X}^n} G^{*n})^{-1} \right)^T \left[(\nabla_{\mathbf{X}^n} I^n)^T + \left(\nabla_{\mathbf{X}^n} G^{*n+1} \right)^T \boldsymbol{\psi}^{n+1} \right], \quad (2.6)$$

in reverse time from $n = N - 1$ to $n = 1$. Note that this technique has already been presented in Rumpfkeil and Zingg (2008).

We adress now the problem of computing $\nabla_{\mathbf{W}} L$. Rather than solve for parameters $\mathbf{W}$ such that $\nabla_{\mathbf{W}} L = 0$ we compute the gradient directly for the current iterative step and

apply a minimization algorithm. The expression for the gradient in its most general form:

$$(\nabla_{\mathbf{W}} L)^T = \begin{pmatrix} (\nabla_{W^1} G^{*1})^T & (\nabla_{W^1} G^{*2})^T & \cdots & (\nabla_{W^1} G^{*N})^T \\ (\nabla_{W^2} G^{*1})^T & (\nabla_{W^2} G^{*2})^T & \cdots & (\nabla_{W^2} G^{*N})^T \\ \vdots & \vdots & \vdots & \vdots \\ (\nabla_{W^P} G^{*1})^T & (\nabla_{W^P} G^{*2})^T & \cdots & (\nabla_{W^P} G^{*N})^T \end{pmatrix} \begin{pmatrix} \psi^1 \\ \psi^2 \\ \vdots \\ \psi^N \end{pmatrix} + \begin{pmatrix} \sum_{n=1}^{N} \frac{\partial I^n}{\partial W^1} \\ \sum_{n=1}^{N} \frac{\partial I^n}{\partial W^2} \\ \vdots \\ \sum_{n=1}^{N} \frac{\partial I^n}{\partial W^P} \end{pmatrix}. \tag{2.7}$$

In this expression, P is equal to the number of distinct parameters. Note that in general most entries $\nabla_{W^i} G^{*j}$ will be equal to zero but this is problem dependent.

The minimization algorithm requires several iterations of the full CFD solution, which itself requires many internal iterations. The procedure is illustrated in Figure 2.1.

2.2.2 Special Cases

Though the formulation and solution of the problem in its most general form has been presented it may be of interest to some readers to take special consideration of some practical cases.

Many fluid flow systems operate for extended periods at steady state. The formulation of section 2.2.1 is simplified by imposing the conditions $N = 1$ and $\frac{\partial}{\partial t}\mathbf{X} = 0$. Explicitly, equation (2.2) becomes:

$$G^* (\mathbf{X}, \mathbf{W}) = G (\mathbf{X}, \mathbf{W}) = 0. \tag{2.8}$$

Using the same procedure as before the solution is easily developed. The recursive system (2.5) and (2.6) is now a much simplified explicit system:

$$\psi = - \left((\nabla_{\mathbf{X}} G)^{-1} \right)^T \nabla_{\mathbf{X}} I, \tag{2.9}$$

and the gradient of the Lagrangian is finally computed:

$$(\nabla_{\mathbf{W}} L)^T = (\nabla_{\mathbf{W}} G^*)^T \psi + (\nabla_{\mathbf{W}} I)^T. \tag{2.10}$$

Of course the treatment of the geometric parameter is no different than the treatment of the control parameter in this case and hence the formulation for the steady state coupled

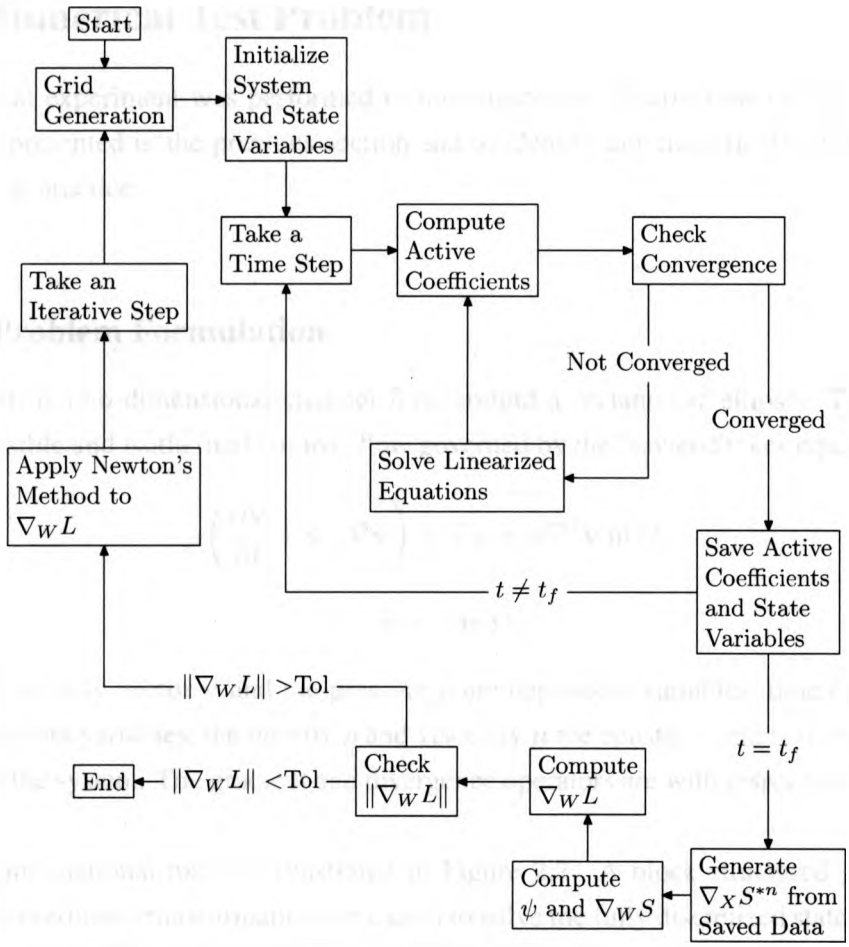

Figure 2.1: Process diagram for the optimization algorithm. The term *active coefficients* refers to the coefficients in front of the dependent variables in the linearized state equations.

optimization problem is no different than the well-established problem of optimizing a dynamical system over multiple control parameters or, similarly, multiple geometric parameters.

Another realistic problem is the optimization of a system subject to a periodic control law of the form $Y_i(t) = g(\mathbf{Y^c}_i, t)$, where $\mathbf{Y^c}_i$ is a P-parameter vector and is independent of time. The formulation for this problem cannot be simplified beyond what has been presented in the general case, Section 2.2.1.

2.3 Numerical Test Problem

A numerical experiment was performed to investigate the effectiveness of the numerical algorithm presented in the previous section and to identify any numerical difficulties that may arise in practice.

2.3.1 Problem Formulation

The system is two dimensional channel flow around a rectangular ellipse. The flow is incompressible and isothermal laminar flow governed by the Navier-Stokes equations:

$$\rho\left(\frac{\partial \mathbf{v}}{\partial t} + \mathbf{v}\cdot\nabla\mathbf{v}\right) + \nabla p = \mu\nabla^2\mathbf{v} \text{ in } \Omega, \tag{2.11}$$

$$\nabla\cdot\mathbf{v} = 0 \text{ in } \Omega, \tag{2.12}$$

where the velocity vector $\mathbf{v}$ and the pressure p are dependent variables, time t and space are independent variables, the density ρ and viscosity μ are constants and Ω is the physical domain of the system. The gradient and divergence operators are with respect to the spatial variables.

The computational mesh is illustrated in Figure 2.2. A block structured grid and a change of coordinate transformation were used to solve the fully discretized state equations at each time step. The transient term was treated implicitly (as in Eq. (2.2)) and deferred pressure correction was used to solve the pressure decoupling problem.

The primary radius r_1 of the ellipse was treated as a geometric variable but the area of the ellipse was fixed. Thus the secondary radius is computed according to $r_2 = \frac{Area}{\pi r_1}$ and hence the geometry is a function of a single parameter. We also allow for suction or blowing across the surface of the ellipse. The spacial profile of the suction/blowing is restricted to a parabolic shape in the η-direction with variable amplitude according to

$$v_{s\eta}(\xi,t) = \frac{(\xi - L_c + r_1)(L_c + r_1 - \xi)}{r_1^2}\alpha(t), \xi \in [L_c - r_1, L_c + r_1], \tag{2.13}$$

where L_c is the ξ-coordinate of the centre of the ellipse and $\alpha(t)$ is the control parameter. Symmetry is also assumed for the suction/blowing profile. Hence the number of control variables is equal to the number of time steps and there is one geometric parameter. In this

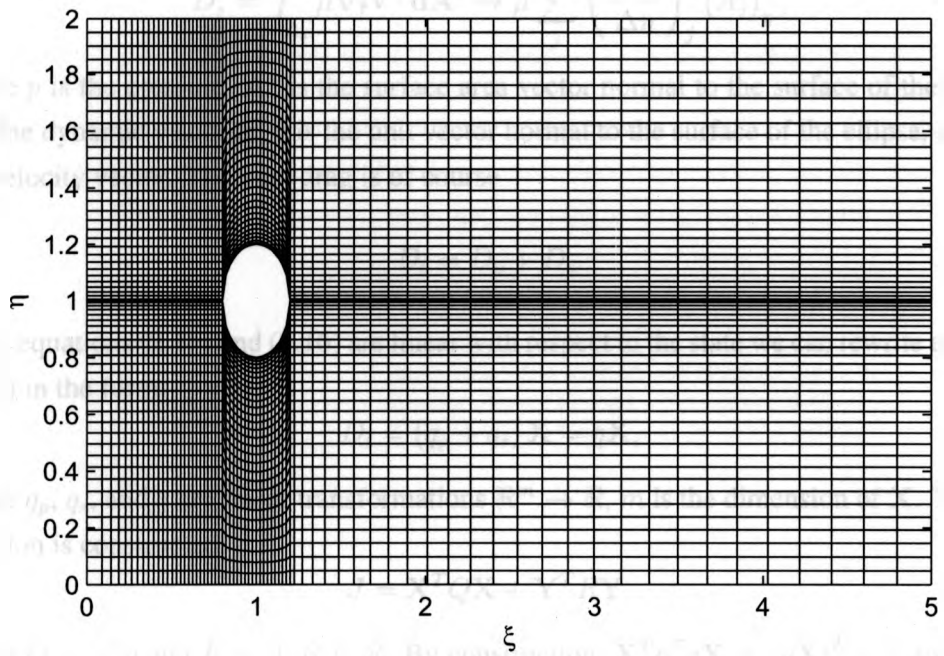

Figure 2.2: Computational mesh for the numerical test problem.

case, equation (2.7) becomes

$$(\nabla_{\mathbf{W}} L)^T = \begin{pmatrix} (\nabla_{Y^1} G^{*1})^T & 0 & \cdots & 0 \\ 0 & (\nabla_{Y^2} G^{*2})^T & \cdots & 0 \\ \vdots & \vdots & \vdots & \vdots \\ 0 & 0 & \cdots & (\nabla_{Y^N} G^{*N})^T \\ (\nabla_Z G^{*1})^T & (\nabla_Z G^{*2})^T & \cdots & (\nabla_Z G^{*N})^T \end{pmatrix} \begin{pmatrix} \boldsymbol{\psi}^1 \\ \boldsymbol{\psi}^2 \\ \vdots \\ \boldsymbol{\psi}^N \end{pmatrix} + \begin{pmatrix} \frac{\partial I^1}{\partial Y^1} \\ \frac{\partial I^2}{\partial Y^2} \\ \vdots \\ \frac{\partial I^N}{\partial Y^N} \\ \sum_{n=1}^{N} \frac{\partial I^n}{\partial Z} \end{pmatrix}. \quad (2.14)$$

The cost function, in this example, is taken as the drag. Two types of drag are considered around the body of the ellipse: pressure drag from the change in momentum across the immersed body and skin friction drag generated from the boundary layer. The discretized drag equations:

$$D_p = \int_{A_s} p \ (dA^s)_\xi \rightarrow \sum_j p_j (A_j^s)_\xi, \quad (2.15)$$

$$D_s = \int_{A_s} \mu \nabla_{\hat{\mathbf{r}}} \mathbf{v} \cdot \mathbf{dA^s} \rightarrow \mu \sum_j \left(\frac{\Delta v_\eta}{\Delta \eta} \right)_j \left(A_j^s \right)_\eta, \tag{2.16}$$

where p is the pressure, $\mathbf{A^s}$ is the surface area vector normal to the surface of the ellipse, μ is the dynamic viscosity, $\hat{\mathbf{r}}$ is the unit vector normal to the surface of the ellipse, and $\mathbf{v}$ is the velocity vector. The total drag is of course

$$D_t = D_p + D_s. \tag{2.17}$$

Since equations (2.15) and (2.16) are linear with respect to the state we can rewrite equation (2.17) in the form:

$$D_t = (q_p + q_s)\,\mathbf{X} = q\mathbf{X}, \tag{2.18}$$

where q_p, q_s, and q are linear transformations $\Re^m \rightarrow \Re$, m is the dimension of $\mathbf{X}$. The cost function is constructed:

$$J = \mathbf{X}^T Q \mathbf{X} + \mathbf{Y}^T R \mathbf{Y}, \tag{2.19}$$

where $Q = q^T q$ and $R > 0$, $R \in \Re$. By construction, $\mathbf{X}^T q^T q \mathbf{X} = (q\mathbf{X})^2 \geq 0$ and hence $J \geq 0$. This ensures that a minimum exists for the system and $R > 0$ prevents a solution where $|\mathbf{Y}|$ is arbitrarily large. Hence a solution must exist for this problem.

The system was coded in Matlab and solved over 648 control volumes with 4 time steps. Though this is a coarse grid for realistic simulation it was sufficient for illustrative purposes. For the minimization algorithm we use a quasi-Newton method for the second order convergence rate and we use the BFGS method (Nocedal and Wright, 2006) to estimate the Hessian. Calculating the gradient $\nabla_{\mathbf{Z}} G$ can be done efficiently and accurately using automatic differentiation (Haslinger and Mäkinen, 2003). However, for simplicity $\nabla_{\mathbf{Z}} G$ was calculated using finite differences from perturbing the computational grid. Though this method requires more computation and temporary data storage it is sufficient for this example. Note that the coefficients are calculated directly for the perturbed grid without having to solve any systems of equations and hence the computational cost is still fairly low.

2.3.2 Control Optimization

The control and geometric optimization problems were each solved separately before solving the coupled optimization problem. The convergence history from the control problem (treating the geometry of the ellipse as a constant) is illustrated in Figure 2.3. There are

two significant observations which can be made from this figure:

- Newton's method converges much faster than the gradient method (as expected).
- The discrete adjoint method reduces the cost function more than the finite difference method does. This suggests that it is a more accurate way to calculate the gradient since it has more accurately determined the minimum using the condition $\nabla L = \mathbf{0}$.

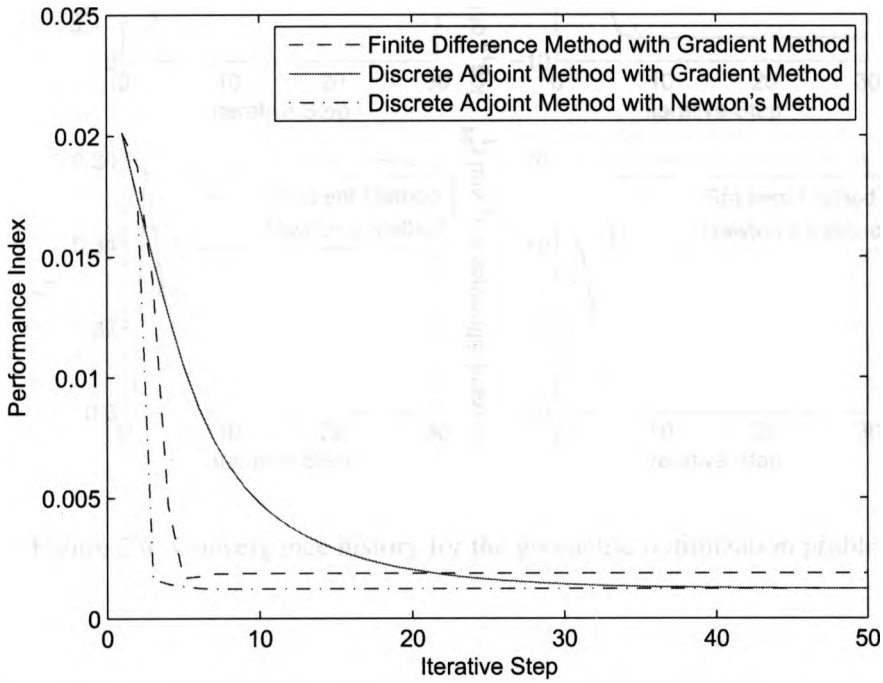

Figure 2.3: Convergence history for the control optimization problem.

2.3.3 Geometric Optimization

The algorithm was also applied in the case when only the geometric variable was changed and no suction or blowing was applied. The initial radius was taken as $r_1^{in} = 0.3$m and the algorithm converged to $r_1^{eq} = 0.32417$m. The results are displayed in Figure 2.4. The oscillation visible in the initial stages with Newton's method is most likely due to a poor estimate of the second derivative resulting from the large initial step lengths.

To investigate whether the equilibrium is in fact a minimum the system was simulated

for a range of values for $Z = r_1$ and the cost function was recorded. The results (Figure 2.5) show that the algorithm has indeed converged to a minimum.

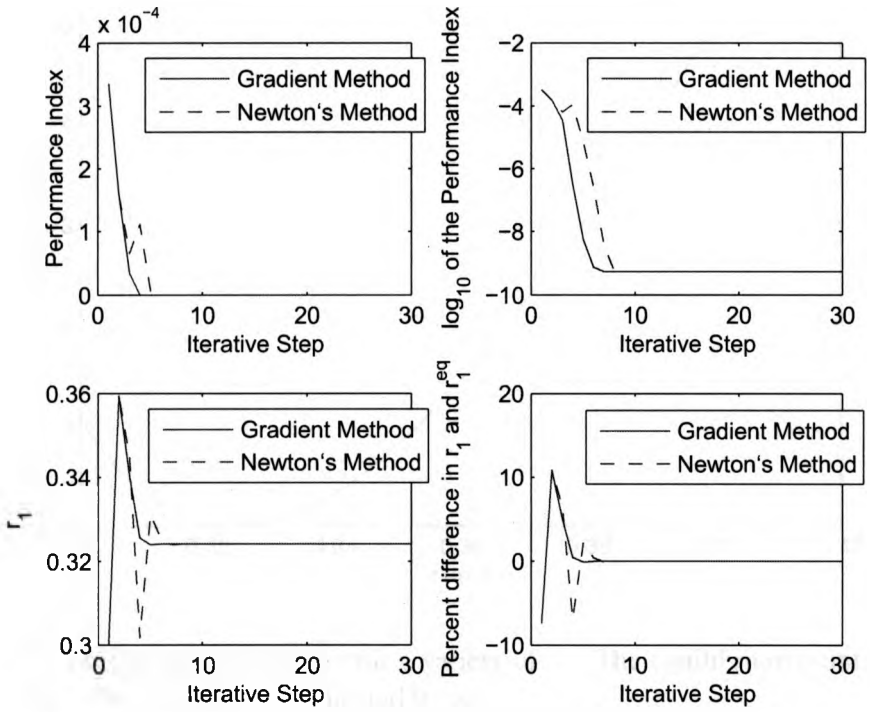

Figure 2.4: Convergence history for the geometric optimization problem.

2.3.4 Coupled Geometric and Control Optimization

The convergence history for the coupled optimization algorithm is provided in Figure 2.6. The final converged value for the performance index from Newton's method is substantially lower than that obtained in either of sections 2.3.2 or 2.3.3.

The profile for J as a function of $\mathbf{W}$ cannot be visualized as it could in section 2.3.3 since J is now a function of several parameters. However, there is no reason to expect that the optimization profile J as a function of its parameters is as simple as it was, for example, in the purely geometric case (Fig. 2.5). This is most likely the reason that the algorithm does not converge smoothly when initialized at $r_1 = 0.3$m and $\mathbf{Y} = \mathbf{0}$, as there may be inflection points and even local minima that will affect convergence between the

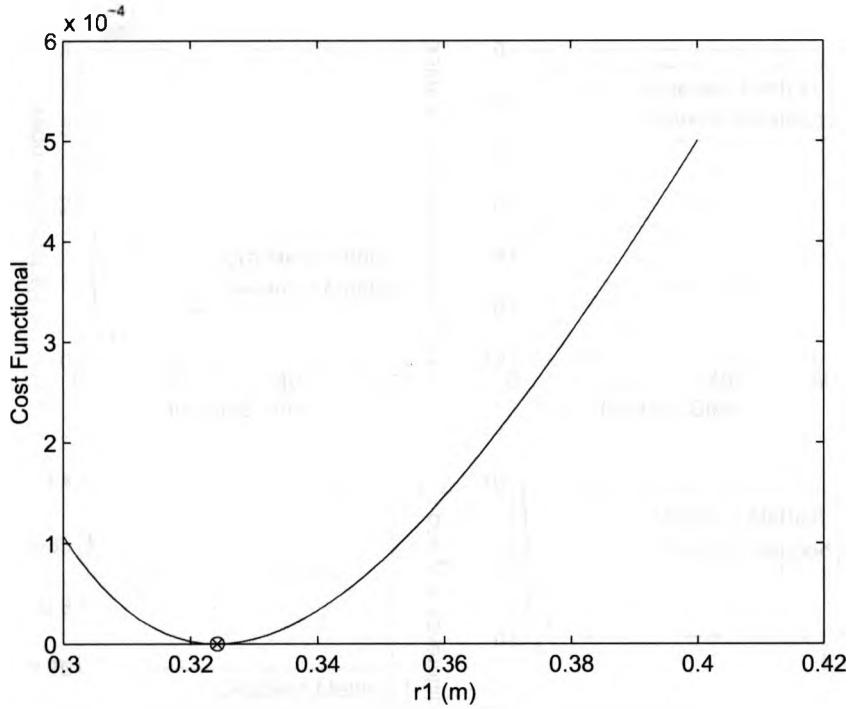

Figure 2.5: Cost function evaluation for a variety of r_1. The equilibrium point generated by the optimization algorithm is indicated by $\otimes$.

initialization point and the global minimum. To improve on this, the system is initialized at the equilibrium from the geometric optimization $r_1^{in} = 0.32417$m and $\mathbf{Y} = \mathbf{0}$ since it is clear from Figures 2.3 and 2.4 that the geometric variable has a much greater impact on performance than the control variable does. The convergence history using this initial data is produced in Figure 2.7.

2.4 Numerical Considerations

The primary benefit of using a discrete adjoint method rather than finite differences to compute ∇J is the reduced computational cost. In this section we briefly discuss how effective this method has been at accomplishing this.

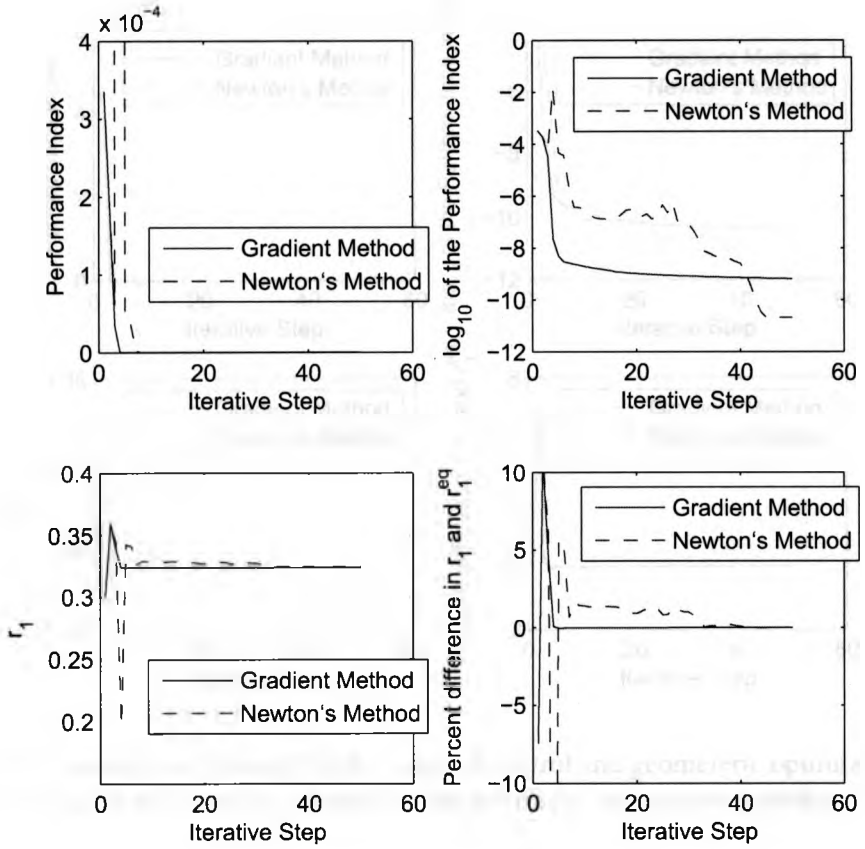

Figure 2.6: Convergence history for the coupled control and geometeric optimization problem.

2.4.1 Computational Cost

We assume that the majority of the computational time is spent solving systems of equations and that the other calculations are small in comparison. The size of the system that must be solved for the CFD solution is $m \times m$, where m is the dimension of $\mathbf{X}$. This system must be solved about $Nk + l$ times, where k is an estimate for the average number of iterations required for convergence at each time step and l is the number of iterations required to initialize the system. Calculating the Lagrangian multipliers then requires the solution of N different $m \times m$ systems. The total number of $m \times m$ systems that must be solved is $(Nk + l + N)\, s$, s being the number of outer iterations required for the optimization process to converge. We observe from this that most of the computational effort at each

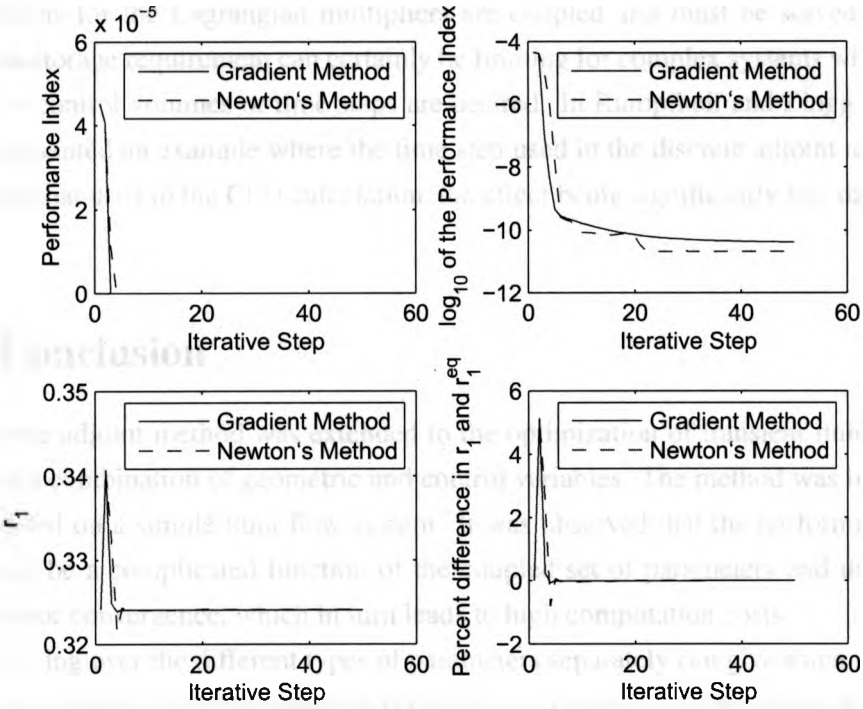

Figure 2.7: Convergence history for the coupled control and geometeric optimization problem with r_1 initialized from the solution to the geometric optimization problem.

iterative step results from solving the state equations, which is regarded as an unavoidable computational necessity, and the discrete adjoint calculation itself provides a significantly smaller contribution to the total computational effort. We observe furthermore that the total computational time depends highly on s, emphasizing once again the importance of a high order optimization algorithm such as Newton's method. Finally, it is observed that the computational cost is essentially independent of the number of system parameters.

2.4.2 Data Storage

In a typical CFD calculation we need only store the coefficients from one time step at a time. The optimization algorithm presented in this paper requires the solution to be stored for all N time steps and hence requires approximately N times more data storage. If the necessary data for the minimization algorithm could be stored progressively after each time step then this could be avoided. This is not possible however with the discrete adjoint method since

the equations for the Lagrangian multipliers are coupled and must be solved in reverse time. This storage requirement can certainly be limiting for complex systems where a large number of control volumes or time steps are desired. In Rumpfkeil and Zingg (2008) the authors presented an example where the time step used in the discrete adjoint method was larger than that used in the CFD calculation, the effect being significantly less data storage.

2.5 Conclusion

The discrete adjoint method was extended to the optimization of transient fluid flow systems with a combination of geometric and control variables. The method was investigated and validated on a simple fluid flow system. It was observed that the performance of the system can be a complicated function of the coupled set of parameters and that this can result in poor convergence, which in turn leads to high computation costs.

Optimizing over the different types of parameters separately can give some insight into the problem. In the case of the example presented in Section 2.3.4, optimizing each parameter type separately indicated that the geometric variable was dominant. Hence, optimizing around this parameter first was useful to get an initialization point for the coupled optimization.

Though the data storage requirements of the discrete adjoint method may be limiting for the most sophisticated CFD systems, the method can be applied to a variety of numerically modeled systems to assist in the engineering design process, or to suggest improvements to an existing design.

References

Haslinger J, Mäkinen RAE (2003) Introduction to Shape Optimization. SIAM

Korivi VM, Taylor III AC, Newman PA, Hou GW, Jones HE (1992) An incremental strategy for calculating consistent discrete sensitivity derivatives. Tech. Rep. NASA TM 104207, NASA Langley Research Center, Hampton,VA

Laporte E, Tallec PL (1999) Numerical Methods in Sensitivity Analysis and Shape Optimization. Springer

Liseikin VV (1999) Grid Generation Methods. Springer

Nocedal J, Wright SJ (2006) Numerical Optimization, Second Edition. Springer

Patankar SV (1980) Numerical Heat Transfer and Fluid Flow. Hemisphere Publishing Corporation

Reuther J, Jameson A (1994) Control theory based airfoil design for potential flow and a finite volume discretization. In: 32nd Aerospace Sciences Meeting and Exhibit, Reno,NV, AIAA-94-0499

Rumpfkeil MP, Zingg DW (2008) The optimal control of unsteady flows with a discrete adjoint method. Optimization and Engineering

Thompson JF, Warsi ZUA, Mastin CW (1985) Numerical Grid Generation: Foundation and Applications. Elsevier Science Publishing Co., Inc.

Chapter 3

Feedback Control of Heat Transfer Systems by the Numerical Method of Lines

3.1 Introduction

The purpose of optimal control is to transition a dynamical system from one point or trajectory to some target state while optimizing some performance index. Since some information from the solution field is necessary to arrive at the optimal control this problem will require the solution over the entire time field using information from the entire spatial field as well.

This paper will assume that the control system cannot be solved by analytical methods. In this case, the entire solution field cannot be predicted a priori and hence the theoretical optimal control cannot be computed directly. Many literature sources in fact use iterative methods to determine the optimal control. There are a variety of well-established minimization procedures available (such as gradient or conjugate gradient methods, or quasi-Newton methods (Nocedal and Wright, 2006) which can be applied directly to the cost functional (Collis et al, 2001) or in association with an adjoint system (Dedè, 2007; Rumpfkeil and Zingg, 2008; Li et al, 2000). Though this method is proven to be effective the control produced is a open loop control.

This paper focuses on a direct approach to feedback optimal control of fluid flow and heat transfer systems. A common tactic in the control of nonlinear dynamical systems is to linearize the state about an equilibrium point and apply a linear control law, such as linear quadratic regulation. In this case, we can guarantee convergence of the system to the equilibrium under the corresponding control law in some non-zero radius, given that the linearized system is controllable (Lee and Markus, 1967). A similar procedure can be adopted for systems governed by partial differential equations with linear transient term by discretizing the spatial variables only. The resulting system is a linear system of differential equations amenable to modern control methods.

The partially discretized system can be very large and solving the resulting control problem generally requires careful consideration of the numerical techniques to be used. We see in Borggaard et al (2004) an optimal control method applied to the Stokes equa-

tions, which is essentially a linearization of the Navier-Stokes equations about the origin, which simplifies the control problem by eliminating the inhomogeneity introduced by the Dirichlet boundary condition. This allows for the control problem to be posed as a linear quadratic regulator problem, which is much more reasonable from a numerical perspective than solving systems of differential equations as we need to do for nonlinear optimal control problems.

In Brown et al (2009) we investigate this control technique and demonstrate that when the linearization point is not equal to the steady state equilibrium point then the control problem will not minimize the cost functional at steady state. This can potentially be amended by linearizing about the current state instead of the origin but the inhomogeneity introduced by this choice of linearization point produces some numerical difficulties for complex systems. In this paper we will investigate the quality of the results produced when linearizing about the current state of the system by numerical simulation on a simple heat transfer system. The dynamics of this particular system depend greatly on inhomogeneous terms.

3.2 Optimal Control of Heat Transfer Systems

This section describes how a fully discretized system can be put into its partially discretized form. An optimal controller is then designed for the partially discretized system. The method is validated through numerical simulation on a simple one-dimensional heat transfer system.

3.2.1 The Numerical Method of Lines

Consider a numerical model for a stationary heat transfer system with temperature as the only dependent variable. In general, the discretization will take the form:

$$a_P T_P = \sum a_{nb} T_{nb} + b_P \tag{3.1}$$

The terms a and b are known as the *active coefficients*.

When dealing with nonlinear systems the usual solution method is to linearize the equations into the above form and resolve any nonlinearities iteratively. Rather than recommence this process at each time step for the partially discretized equations it is preferable

to develop them in terms of the fully discretized equations. Assume that the system is first order and linear with respect to the transient term. Assume furthermore that the system has been discretized using implicit time integration. Then without loss of generality, consider the specific transformation to the transient term for the system that will be studied in this paper:

$$M_P \frac{\partial T_P}{\partial t} \rightarrow M_P \frac{T_P - T_P^O}{\Delta t}. \tag{3.2}$$

Note that such a transformation is *not* invertible, but if we know how the original partial differential equation has been discretized then it is a simple matter to reverse this transformation. The reverse transformation is given by:

$$M_P \frac{T_P - T_P^O}{\Delta t} \rightarrow M_P \frac{\partial T_P}{\partial t}. \tag{3.3}$$

This results in the following equation:

$$\frac{\partial T_P}{\partial t} = \frac{1}{M_P}\left(\frac{M_P}{\Delta t} - a_P\right) T_P + \frac{1}{M_P} \sum a_{nb} T_{nb} + \frac{1}{M_P}\left(b_P - \frac{M_P}{\Delta t} T_P^O\right). \tag{3.4}$$

These equations can be written in compact form:

$$\frac{\partial T_P}{\partial t} = c_P T_P + \sum c_{nb} T_{nb} + d_P. \tag{3.5}$$

The coefficients c and d will be referred to henceforth as the *control active coefficients*.

3.2.2 Optimal Control

Consider a heat transfer system with partial discretization of the form

$$\dot{T} = f\left(T(t), u(t)\right)$$

where u is the control vector. Consider the control problem of driving the temperature at some location in the system to specified terminal condition T_f while minimizing the cost functional $J = \int_{t_0}^{t_f} f_0\left(T(t), u(t)\right)\, dt$. Adjoining the state to this cost function using the multiplier function $\psi(t)$:

$$J = \int_{t_0}^{t_f} \left[f_0(T(t), u(t)) + \psi^T(t) \left\{ f(T(t), u(t)) - \dot{T}(t) \right\} \right] dt. \tag{3.6}$$

Note that $\psi(t)$ is assumed to be a vector of differentiable real-valued functions. The following quantity is known as the *first variation of J*:

$$\delta J = \left[-\psi^T \delta T\right]_{t=t_f} + \int_{t_0}^{t_f} \left[\left(\frac{\partial H}{\partial T} + \dot{\psi}^T\right)\delta T + \frac{\partial H}{\partial u}\delta u\right] dt. \tag{3.7}$$

Above, δT and δu are small perturbations on T and u respectively. To simplify the notation, the scalar function H was introduced. This quantity is known as the *Hamiltonian* and it is defined as:

$$H(T(t), u(t), \psi(t)) = f_0(T(t), u(t)) + \psi^T(t) f(T(t), u(t)). \tag{3.8}$$

As it turns out, a necessary condition for J to be a minimum is $\delta J = 0$ for any δT, δu (Bryson and Ho, 1969; Pinch, 1993). This can be achieved by appropriate assignment of the multiplier functions:

$$\dot{\psi}^T = -\frac{\partial H}{\partial T} = -\frac{\partial f_0}{\partial T} - \psi^T \frac{\partial f}{\partial T}, \tag{3.9}$$

$$\psi^T(t_f) = 0, \tag{3.10}$$

$$\frac{\partial H}{\partial u} = 0. \tag{3.11}$$

Equations (3.9), (3.10), and (3.11) are known as the *Euler-Lagrange* equations. Moreover, if $T_i(t_f)$ is a desired condition, then clearly $\delta T_{t_f} = 0$ and so the boundary condition $\psi_i(t_f) = 0$ can be replaced by $T_i(t_f)$.

3.2.3 The Heated Rod and its Partial Discretization

Consider a solid, horizontal, stationary rod with constant cross-sectional area experiencing internal conduction and external convection. Note that this system is intrinsically linear. Consider as well the control problem of guiding the temperature of the tip of the rod to a specified final temperature T_f at time t_f while minimizing the cost functional $\int_{t_0}^{t_f} \frac{1}{2}u^2\, dt$. The control is the heat input at the root. That is, $u = \dot{q}$. The control system is depicted in Figure 3.1.

Some special attention needs to be given in this case to the endpoints. Since the nodes at both ends are taken on the outer face of the rod these nodes do not correspond to an individual control volume and hence there is no mass associated with either of them. As a result, the transient term vanishes on these nodes.

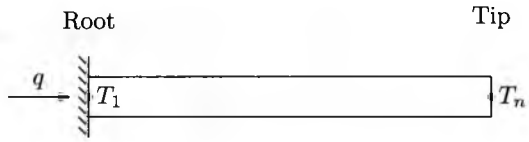

Figure 3.1: The configuration of the heated rod

At the west face the discrete equation is of the form:

$$a_{P1}T_1 = a_{E1}T_2 + b_1 + \dot{q}. \tag{3.12}$$

At the east face the discrete equation is of the form:

$$a_{Pn}T_n = a_{Wn}T_{n-1} + b_n. \tag{3.13}$$

To develop these equations into the partially discretized system substitute them into the equations for the neighbouring nodes. This will eliminate the terms T_1 and T_n from the system. The details are omitted here. The final partially dicretized system equations are represented here in compact form:

$$\frac{\partial T_i}{\partial t} = \begin{cases} c_{Pi}T_i + c_{Ei}T_{i+1} + d_{Pi} + c_u\dot{q}, & i = 2; \\ c_{Pi}T_i + c_{Ei}T_{i+1} + c_{Wi}T_{i-1} + d_{Pi}, & i = 3 \ldots n-2; \\ c_{Pi}T_i + c_{Wi}T_{i-1} + d_{Pi}, & i = n-1. \end{cases} \tag{3.14}$$

3.2.4 Optimal Control of the Heated Rod System

Consider the system presented in the previous section. The Hamiltonian for the system is given by:

$$\begin{aligned} H = f_0 &+ \psi_2 f_2 + \psi_3 f_3 + \cdots + \psi_{n-1} f_{n-1} \\ = \frac{1}{2}u^2 &+ (c_{P2}T_2 + c_{E2}T_3 + d_2 + c_u u(t))\,\psi_2 \\ &+ (c_{P3}T_3 + c_{W3}T_2 + c_{E3}T_4 + d_4)\,\psi_3 \\ &+ \cdots + \\ &+ (c_{Pi}T_i + c_{Wi}T_{i-1} + c_{Ei}T_{i+1} + d_i)\,\psi_i \\ &+ \cdots + \\ &+ (c_{Pn-1}T_{n-1} + c_{Wn-1}T_{n-2} + d_{n-1})\,\psi_{n-1}. \end{aligned} \tag{3.15}$$

The third Euler-Lagrange equation (Eqn. (3.11)) gives:

$$\begin{aligned} & \frac{\partial H}{\partial u} = u + c_u \psi_2 = 0 \\ \Rightarrow \quad & u = -c_u \psi_2 \end{aligned} \tag{3.16}$$

Substituting this back into the original ODE system, the equation at the first interior node becomes:

$$\frac{\partial T_2}{\partial t} = c_{P2} T_2 + c_{E2} T_3 + d_{P2} - c_u^2 \psi_2. \tag{3.17}$$

The first set of Euler-Lagrange equations (Eqns. (3.9)) are known as the *adjoint* or *costate* equations. For the heated rod system, these equations become:

$$\dot{\psi}_i = \begin{cases} -c_{Pi}\psi_i - c_{W(i+1)}\psi_{i+1}, & i = 2; \\ -\psi_{i-1}c_{E(i-1)} - \psi_i c_{Pi} - \psi_{i+1}c_{W(i+1)}, & i = 3, \ldots, n-2; \\ -c_{E(i-1)}\psi_{i-1} - c_{Pi}\psi_i, & i = n-1. \end{cases} \tag{3.18}$$

There are $n-2$ state equations and $n-2$ adjoint equations. There are $n-2$ initial conditions on the state equations. There is one terminal condition on variable T_n and $n-3$ terminal conditions on the adjoint multipliers. Hence, the problem is fully determined. However, the variable T_n does not appear explicitly in any of these equations and so the terminal condition on this variable must be transferred over to the term T_{n-1}. Explicitly:

$$\begin{aligned} & T_n(t_f) = T_f = \frac{a_{Wn}}{a_{Pn}} T_{n-1} + \frac{b_n}{a_{Pn}} \\ \Rightarrow \quad & T_{n-1}(t_f) - \frac{a_{Pn}}{a_{Wn}} \left(T_f - \frac{b_n}{a_{Pn}} \right) = 0. \end{aligned} \tag{3.19}$$

3.2.5 Quadratic Regulation

Terminally constrained control problems are not very useful in practice because they do not ensure good performance after the control objective has been met. That is, the control law does not anticipate the system behaviour after $t = t_f$. Rather than specifying a terminal temperature at the tip, it is more effective to penalize the quadratic term $\frac{1}{2}(T_n - T_f)^2$. Making this term quadratic forces it to be positive or zero, which ensures well-posedness of the control problem. Since this term will compete with the cost associated with u it is appropriate to attach a multiplier to this term, denoted α.

The new control problem is to minimize:

$$J = \int_{t_0}^{t_f} \frac{\alpha}{2} (T_n - T_f)^2 + \frac{1}{2} u^2 \, dt, \tag{3.20}$$

with no terminal constraints. Expanding the above expression for J and substituting in the algebraic expression for T_n simplifies to:

$$J = \gamma (t_f - t_0) + \int_{t_0}^{t_f} \left(\beta_1 T_{n-1}^2 + \beta_2 T_{n-1} + \frac{1}{2} u^2 \right) dt, \tag{3.21}$$

where γ, β_1, and β_2 are constants. Since $J > 0$ then $J - \gamma (t_f - t_0)$ is bounded below and hence minimization of $J - \gamma (t_f - t_0)$ is still well-posed for fixed endpoint problems where $t_f > t_0$ and t_f is finite. Hence, take $J - \gamma (t_f - t_0)$ as the cost functional.

The Hamiltonian for the system:

$$H = \beta_1 T_{n-1}^2 + \beta_2 T_{n-1} + \frac{1}{2} u^2 + \psi_2 f_2 + \ldots + \psi_i f_i + \ldots + \psi_{n-1} f_{n-1}. \tag{3.22}$$

The third Euler-Lagrange equation (Eqn. (3.11)) still gives $u = -c_u \psi_2$. Only the last costate equation differs from those developed in the previous subsection:

$$\dot{\psi}_{n-1} = -\frac{\partial H}{\partial T_{n-1}} = -2\beta_1 T_{n-1} - \beta_2 - c_{En-2}\psi_{n-2} - c_{Pn-1}\psi_{n-1}. \tag{3.23}$$

Choice of the weighting parameter α will greatly affect the results. Larger α will emphasize minimization of $(T_n - T_f)^2$ and smaller α will emphasize minimization of u^2.

3.2.6 Numerical Results for the Linear Time-Invariant (LTI) Case

The heated rod system as described is an LTI system. The control problem was simulated in MATLAB according to the process diagram in Fig. 3.2. The results and observations are presented in this section.

The rod is initially at room temperature of 283K. The control objective is to choose $u(T(t))$ that will minimize the cost functional given by Eqn. (3.20) with T_f =288K. For repeatability the physical parameters of the system are mentioned here: $\rho = 1000 \text{kg m}^{-3}$, $k = 20 \text{Wm}^{-1}\text{K}^{-1}$, $C_p = 500 \text{J kg}^{-1}\text{K}^{-1}$, $h = 50 \text{Wm}^{-2}\text{K}^{-1}$, $A_c = 2.5 \times 10^{-5} \text{m}^{-2}$, $L = 0.1 \text{m}$. The rod has a square cross section.

Choice of the weighting parameter α has a drastic impact on the system behaviour. If

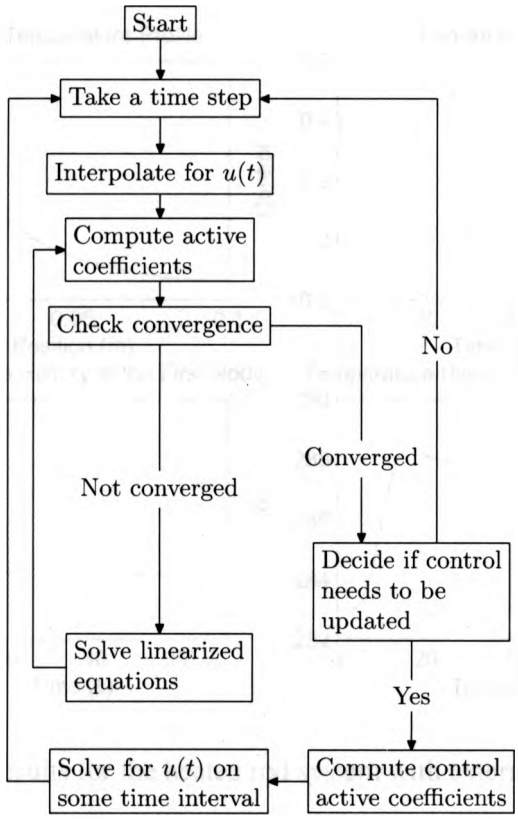

Figure 3.2: Process diagram for application of a feedback control law to a CFD system

α is large then the control objective is emphasized. This will ensure that the condition $T_n = T_f$ is met rapidly but may result in large overshoot. If α is small then the control cost is emphasized. This will generally reduce the magnitude of the control law but may result in slow convergence or an equilibrium that is below the control objective. Some trial and error indicated that $\alpha = 0.001$ is a reasonable value. Figure 3.3 shows good performance.

The problem of controlling LTI fluid flow systems is rather trivial as the linearization is not time-dependent. The problem of controlling nonlinear systems is significantly more difficult. The results are presented in the following section.

3.2.7 Optimal Control of Nonlinear Systems under FVM

Dynamical systems have often been controlled with optimal control by linearizing about an equilibrium point and developing the control for the linearized system. This control is stabilizing for the nonlinear system if the linearization is controllable. Unfortunately

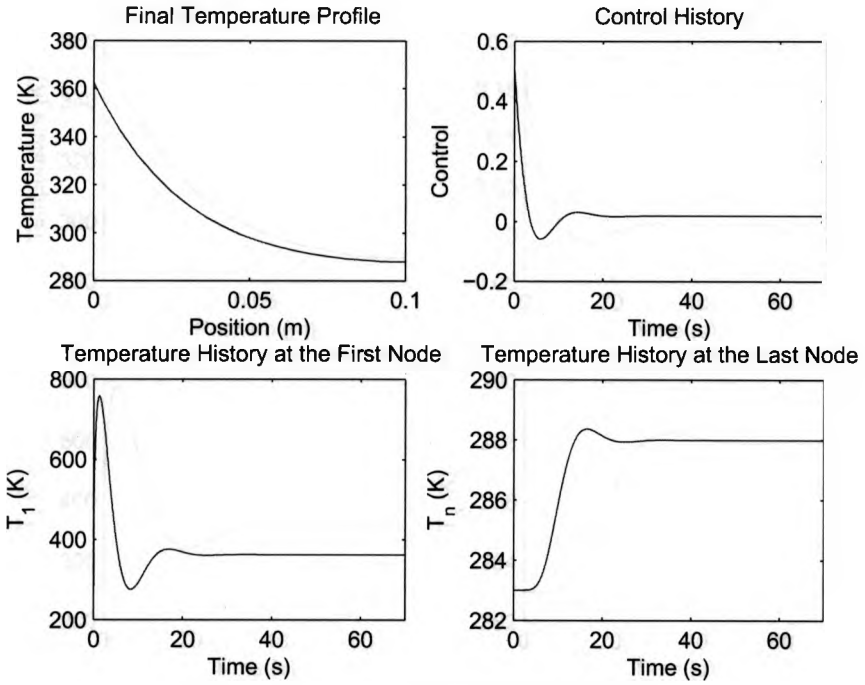

Figure 3.3: Numerical results for the heated rod system with external convection and internal conduction

the problem is more difficult in CFD. If the solution field was known, numerical methods (such as FVM) would be unnecessary, and hence the solution field must be assumed to be unknown for CFD problems. In effect, a linearization at the equilibrium point is not available. However, the resolved dynamics at each time step can be treated as a local linearization for the system and the control can be generated based on that information. Since this linearization will evolve with time the control will no longer be the theoretical optimal control to the infinite-horizon control problem but rather a "best estimate" for what that control should be. This estimate must be updated at regular time intervals until equilibrium is reached.

Nonlinearity is introduced into the heated rod system described in this paper by including a radiation term $\sigma A_c T_P^4$ into the governing equations. The standard procedure for solving the discretized equations according to the finite volume method is to solve the discretized equations iteratively, updating T_P at each time step, until the solution is converged. Once a converged solution is reached Eqn. (3.4) can be applied to determine the partially discretized equations. The optimal control is then developed from the partially discretized

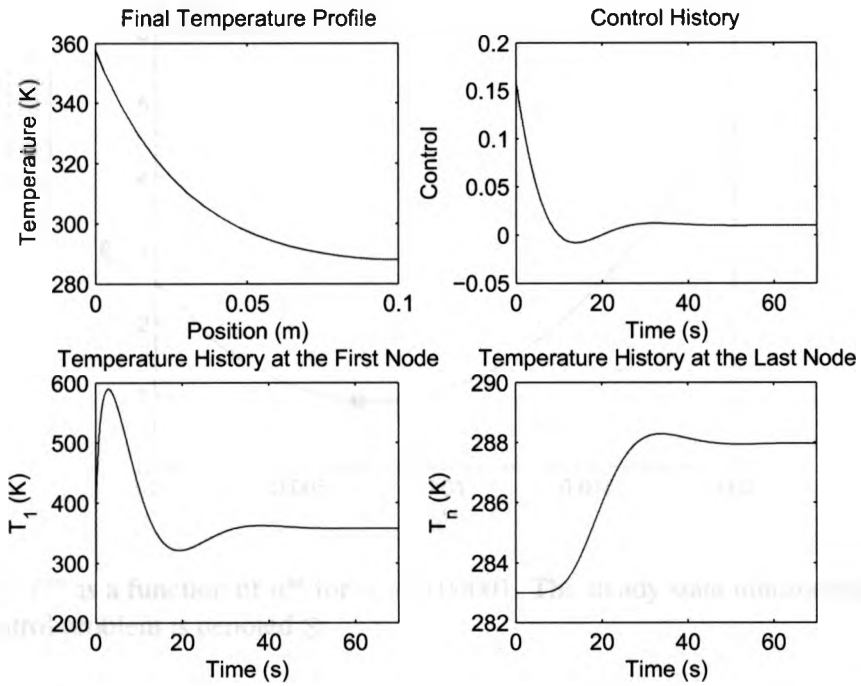

Figure 3.4: Numerical results for the heated rod system with external convection, internal conduction and radiation

system as before.

If we linearize this system about the origin then by analysis the radiation term is small and can be neglected. However, the equilibrium point in this case is not the origin but is in the hundreds of degrees Kelvin, so this linearization will present a very poor approximation to the system. A more suitable linearization point in this case is the current state of the system. Hence, this problem is a good illustration for the method of this paper.

3.2.8 Numerical Results for the Nonlinear Case

The numerical simulation for the heated rod with radiation was carried out with the same physical parameters as were used for the linear case. The results for the nonlinear system are displayed in Fig. 3.4. Not surprisingly, the results are similar to what was observed in Fig. 3.3.

Though it is clear from Fig. 3.4 that the results have converged to the control objective,

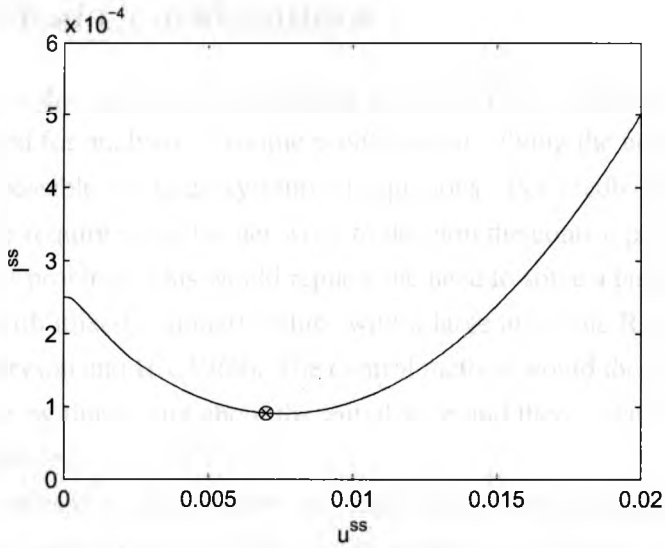

Figure 3.5: I^{ss} as a function of u^{ss} for $\alpha = 0.00001$. The steady state minimum generated by the control problem is denoted $\otimes$.

we wish to verify that the control results have indeed minimized the cost functional at steady state. The cost functional at any time after steady state is reached is given by:

$$J^{ss} = \frac{1}{2}\int_t^\infty \alpha\,(T_n^{ss} - T_f)^2 + (u^{ss})^2 \,\mathrm{d}\tau. \tag{3.24}$$

Since the integrand is constant, minimizing the cost functional at steady state is equivalent to minimizing the quantity:

$$I^{ss} = \alpha\,(T_n^{ss} - T_f)^2 + (u^{ss})^2\,. \tag{3.25}$$

Hence, it is expected that the quantity I^{ss} should be minimized at steady state.

To investigate whether or not this is the case, we select α in such a way that $T_n \neq T_f$ at steady state. Selecting $\alpha = 0.00001$ gives a steady state solution of $T_n^{ss} = 286.48$, $u^{ss} = 0.007$, $I^{ss} = 0.000072$. The steady state solution field was generated by solving the system to steady state for a variety of u^{ss}. The results are plotted in Fig. 3.5.

3.3 Numerical Considerations

The control law in this paper was developed directly from variational principles. This method can be used for analysis of simple problems but solving the necessary differential equations is not possible for large systems of equations. For feedback control of large-scale problems we require some further work to develop the control problem into a linear quadratic regulator problem. This would replace the need to solve a large system of differential equations with mixed boundary values with a large algebraic Ricatti form equation (Brocket, 1969; Bryson and Ho, 1969). The control method would then be to initialize the control law offline by linearizing about the initial state and then update the law at regular intervals as the state evolves.

Though this problem remains numerically challenging many advanced numerical techniques exist for the solution of this problem such as Penzl (1999), which is presently available from http://www.tu-chemnitz.de/sfb393/lyapack/. Unfortunately this reformulation of the problem can be a challenging task depending on the properties of the governing partial differential equations of the system.

3.4 Concluding Remarks

The mathematical formulation for the control problem presented in this paper is demonstrated to be effective for dynamical systems governed by either linear or nonlinear partial differential equations. In the example presented the control system converged to a local steady state minimum when the current state was selected as the linearization point. Further work is required to reduce the numerical challenges of the problem before the control law can be implemented as a real time feedback law.

References

Borggaard J, Burns J, Zietsman L (2004) Computational challenges in control of partial differential equations. In: 2nd AIAA Flow Control Conference

Brocket RW (1969) Finite Dimensional Linear Systems. John Wiley & Sons, Inc.

Brown D, Zhang C, Jiang J (2009) Optimal feedback control of the Navier-Stokes equations. In: 20th International Symposium on Transport Phenomena

Bryson AE, Ho YC (1969) Applied Optimal Control. Blaisdell Publishing Company

Collis SS, Ghayour K, Heinkenschloss M, Ulbrich M, Ulbrich S (2001) Optimal control of unsteady compressible viscous flows. International Journal for Numerical Methods in Fluids 40

Dedè L (2007) Optimal flow control for Navier-Stokes equation: Drag minimization. International Journal for Numerical Methods in Fluids 55:347–366

Lee EB, Markus L (1967) Foundations of Optimal Control Theory. J. Wiley and Sons

Li Z, Navon IM, Hussaini MY, Le Dimet FX (2000) Optimal control of the unsteady Navier-Stokes equations. Computers & Fluids 32

Nocedal J, Wright SJ (2006) Numerical Optimization, Second Edition. Springer

Penzl T (1999) LyaPack Users' Guide (Version 1.0). Available at http://www.netlib.org/lyapack/guide.pdf

Pinch ER (1993) Optimal Control and the Calculus of Variations. Oxford University Press Inc.

Rumpfkeil MP, Zingg DW (2008) The optimal control of unsteady flows with a discrete adjoint method. Optimization and Engineering

Chapter 4

Linear Quadratic Feedback Control of Incompressible Fluid Flow Systems with the Finite Volume Method

4.1 Introduction

This paper addresses the problem of optimal feedback control of dynamical systems that are governed by nonlinear partial differential equations. This subject has been approached from many different directions in recent years. A good summary of the recent progress is provided in Gad-el-Hak and Bewley (2006). This paper is specifically concerned with the application of feedback control laws to numerically simulated incompressible fluid flow systems where the finite volume discretization is employed. The approach taken in this paper is to first discretize the system spacially using the finite volume technique and then apply the control law to the resulting system of ordinary linear differential equations. Though the feedback control problem has been addressed in the past for the finite element method in Stoyanov (2006), the discretized system takes on a more difficult form when the finite volume method is used. Optimal control of ordinary differential equations has been studied extensively in the literature and some early but complete texts on the subject include Bryson and Ho (1969) and Brocket (1969).

Application of control laws to the discretized Navier-Stokes equations presents some unique challenges. To illustrate this the Navier-Stokes equations are produced here:

$$\rho\left(\frac{\partial \boldsymbol{v}}{\partial t} + \boldsymbol{v}\cdot\nabla\boldsymbol{v}\right) + \nabla p = \mu\nabla^2\boldsymbol{v} \text{ in } \Omega, \tag{4.1}$$

$$\nabla\cdot\boldsymbol{v} = 0 \text{ in } \Omega, \tag{4.2}$$

where the velocity vector $\boldsymbol{v}$ and the pressure p are dependent variables, time t and space are independent variables, the density ρ and viscosity μ are constants and Ω is the physical domain of the system. The gradient and divergence operators are with respect to the spatial variables.

Equations (4.1) and (4.2) are discretized spatially according to the finite-volume method. The control $\mathbf{u}$ is applied on some subset of the computational domain Ω. The discretized

control system takes the form:

$$E\dot{\mathbf{x}} = A\mathbf{x} + B\mathbf{u},\ E = \begin{pmatrix} E_1 & 0 \\ 0 & 0 \end{pmatrix},\ A = \begin{pmatrix} A_{11} & A_{12} \\ A_{21} & 0 \end{pmatrix}, \tag{4.3}$$

where $\mathbf{x}$ is the state including both presure and velocity terms and E and A are matrices. Note that systems of this form with E singular (as is the case here) are known as degenerate control systems. This could equivalently be treated as a coupled system of differential and algebraic equations, known as a differential algebraic equation. Furthermore, the form of A in this case does not allow for the algebraic part to be eliminated from the equation.

One control strategy when considering laminar two-dimensional channel flow is to write eqs. (4.1) and (4.2) in a divergence-free basis ($\nabla \cdot \mathbf{v} = 0$) to eliminate the pressure. The Fourier transform is then applied and, with some work, the Orr-Somerfeld/Squire equations are developed (Drazin, 2002). Control techniques can then be applied to the system in the frequency domain (Högberg et al, 2003). Sadly this method is limited to certain geometries and furthermore the treatment of the boundary conditions through this process can be rather tricky (Gad-el-Hak and Bewley, 2006).

Solving the control problem in a divergence-free basis is known as a centralized approach. This paper will focus on the decentralized approach, which requires the direct treatment of system (4.3). This problem is formulated as a linear quadratic regulator (LQR) problem; an objective function J is specified to be minimized which is quadratic with respect to both the state $\mathbf{x}$ and control $\mathbf{u}$. Such problems have been studied by Borggaard et al (2004) and Stoyanov (2006).

The dissertation Stoyanov (2006) provides a full analysis and derivation for the linear quadratic regulator law when the finite element discretization technique is employed. However, it may be observed that there is a critical difference between the finite element and finite volume discretization: when the finite element discretization is employed, the relation $A_{21} = A_{12}^T$ holds but no such relationship exists for the finite volume method. Thus, the optimal control problem for the finite volume discretized system takes on a more general form than the finite element discretized system. Since many modern computational fluid dynamics (CFD) programs use the finite volume method it is practical to develop the LQR law for this condition. In the following section, the LQR control law will be developed from first principles proceeding in a similar way as was presented in Stoyanov (2006) but without the assumption $A_{21} = A_{12}^T$.

4.2 Background, Formulation, and Derivation

Linear quadratic regulation has long been established as an effective means for control of linear and also nonlinear systems. There is a wide variety of literature on the subject. Hence, the amount of detail presented in this section is limited to what is relevant to this paper. A thorough treatment of the material on optimal control is presented in Bryson and Ho (1969). In this section, the LQR problem will be investigated in the general case and the feedback law will be derived for some special cases by methods similar to what has been done in Stoyanov (2006). Since these equations are too complex to solve either analytically or numerically, an alternative solution strategy is used to develop the feedback law and the solution is investigated numerically as a legitimate solution to the original LQR problem.

4.2.1 Optimal Control

The optimal control problem is formulated as the minimization problem: *minimize the cost functional* $J = \int_{t_0}^{t_f} f_0\left(\mathbf{x}(t), \mathbf{u}(t)\right)\, dt$ *subject to constraints* $f\left(\mathbf{x}(t), \mathbf{u}(t)\right) = 0$, where $f = 0$ are the state equations. This is a standard variational calculus problem and it is approached by first appending the state equations onto the cost functional. The resulting quantity, denoted L, is referred to as the *Lagrangian*. Explicitly:

$$L = \int_{t_0}^{t_f} \left[f_0\left(\mathbf{x}(t), \mathbf{u}(t)\right) + \psi^T(t) f\left(\mathbf{x}(t), \mathbf{u}(t)\right)\right]\, dt. \tag{4.4}$$

The unknown functions $\psi(t)$ are referred to as *Lagrangian multipliers*. Note that $\psi(t)$ is assumed to be a vector of differentiable real-valued functions. Taking small perturbations in the direction $\delta \boldsymbol{u}$ produces perturbations $\delta \boldsymbol{x}$ in the state variables. Applying a small perturbation $\delta \boldsymbol{u}$ to the Lagrangian ultimately produces the following equation, known as the *first variation of* L:

$$\delta L = \left[-\psi^T \delta \mathbf{x}\right]_{t=t_f} + \int_{t_0}^{t_f} \left[\left(\nabla_{\mathbf{x}} H + \dot{\psi}^T\right) \delta \mathbf{x} + \nabla_{\mathbf{u}} H \delta \mathbf{u}\right]\, dt. \tag{4.5}$$

To simplify the notation, the scalar function H was introduced. This quantity is known as the *Hamiltonian* and it is defined as:

$$H(\mathbf{x}(t), \mathbf{u}(t), \psi(t)) = f_0(\mathbf{x}(t), \mathbf{u}(t)) + \psi^T(t) f(\mathbf{x}(t), \mathbf{u}(t)). \tag{4.6}$$

As it turns out, a necessary condition for J to be a minimum is $\delta L = 0$ for any $\delta\mathbf{x}$, $\delta\mathbf{u}$ (see, for instance, Bryson and Ho (1969) or Pinch (1993)). This can be achieved by appropriate assignment of the multiplier functions:

$$\dot{\boldsymbol{\psi}}^T = -\nabla_{\mathbf{x}} H = -\nabla_{\mathbf{x}} f_0 - \boldsymbol{\psi}^T \nabla_{\mathbf{x}} f, \tag{4.7}$$

$$\boldsymbol{\psi}^T(t_f) = 0, \tag{4.8}$$

$$\nabla_{\mathbf{u}} H = 0. \tag{4.9}$$

Equations (4.7), (4.8), and (4.9) are known as the *Euler-Lagrange* equations. Moreover, if $\boldsymbol{x}_i(t_f) = \boldsymbol{x}_i^*$ is a desired condition, then clearly $\delta\boldsymbol{x}_{t_f} = 0$ and so the boundary condition $\boldsymbol{\psi}_i(t_f) = 0$ can be replaced by $\boldsymbol{x}_i(t_f) = \boldsymbol{x}_i^*$.

4.2.2 Linear Quadratic Regulation

The linear quadratic regulator (LQR) problem is the special case of optimal control where the cost functional takes on the form:

$$J = \frac{1}{2}\int_0^\infty \left[\mathbf{x}^T Q\mathbf{x} + 2\mathbf{x}^T N\mathbf{u} + \mathbf{u}^T R\mathbf{u}\right]\, dt \tag{4.10}$$

subject to the system dynamics given by equations:

$$E\dot{\mathbf{x}} = A\mathbf{x} + B\mathbf{u} + C. \tag{4.11}$$

The case where E is invertible is well-established. Pre-multiplying each side of eq. (4.11) by E^{-1} will reduce the problem to an equivalent system for which $E = I$ (where I is the identity matrix). The control law has an explicit analytical solution under this condition:

$$\mathbf{u} = -R^{-1}\left[\left(B^T P + N^T\right)\mathbf{x} + B^T\mathbf{k}\right], \tag{4.12}$$

where P is given implicitly as the solution to the algebraic Riccati equation

$$PA + A^T P - (PB + N)\, R^{-1}\left(B^T P + N^T\right) + Q = 0, \tag{4.13}$$

and $\mathbf{k}$ is given by the expression

$$\left[(N + PB)\, R^{-1} B^T - A^T\right]\mathbf{k} = PC. \tag{4.14}$$

Equation (4.13) is a challenging nonlinear matrix algebraic equation which has been studied extensively in the literature and for which many numerical solution methods are available. Solving eq. (4.14) is a simple matter once the solution to eq. (4.13) is obtained.

Though optimal control problems are widely studied in the literature most applications have not required the formulation for inhomogeneous linear systems and the inclusion of the term N in the cost functional is uncommon. Therefore, a brief derivation of eqs. (4.12-4.14) is included here.

Assume that $E = I$. The Hamiltonian of this control problem according to eq. (4.6) is

$$H = \frac{1}{2}\mathbf{x}^T Q\mathbf{x} + \mathbf{x}^T N\mathbf{u} + \frac{1}{2}\mathbf{u}^T R\mathbf{u} + \boldsymbol{\psi}^T \left(A\mathbf{x} + B\mathbf{u} + C\right). \tag{4.15}$$

Direct substitution of H into eq. (4.9) gives

$$\mathbf{u} = -R^{-1}\left(B^T\boldsymbol{\psi} + N^T\mathbf{x}\right) \tag{4.16}$$

and substitution of eqs. (4.16) and (4.15) into eq. (4.7) gives

$$\dot{\boldsymbol{\psi}} = \left(-Q + NR^{-1}N^T\right)\mathbf{x} + \left(NR^{-1}B^T - A^T\right)\boldsymbol{\psi}. \tag{4.17}$$

Assume now that $\boldsymbol{\psi}$ takes the form $\boldsymbol{\psi} = P\mathbf{x} + \mathbf{k}$. Substituting this into eq. (4.17) and performing some tedious algebra results in the equation

$$\begin{aligned}\left[PA + A^TP - (PB + N)\,R^{-1}\left(B^TP + N^T\right) + Q\right]\mathbf{x}(t) \\ = \left[(N + PB)R^{-1}B^T - A^T\right]\mathbf{k} - PC.\end{aligned} \tag{4.18}$$

Setting $\boldsymbol{k}$ according to eq. (4.14) induces

$$\left[PA + A^TP - (PB + N)\,R^{-1}\left(B^TP + N^T\right) + Q\right]\mathbf{x}(t) = 0. \tag{4.19}$$

Since this must be true for all $\mathbf{x}(t)$ and $\mathbf{x}(t)$ is continuous and not uniformly 0, eq. (4.13) results.

4.2.3 State-Costate System for the Discretized Navier-Stokes Equations

The unusual form of the discretized Navier-Stokes equations requires some special treatment and cannot be generalized from the usual Riccati formulation of the LQR problem. In this section the state-costate system is derived from first principles.

Consider the problem of minimizing the cost functional

$$J = \frac{1}{2}\int_0^\infty \left[\boldsymbol{v}^T(\tau)Q_v\boldsymbol{v}(\tau) + \boldsymbol{p}^T(\tau)Q_p\boldsymbol{p}(\tau) + \boldsymbol{u}^T(\tau)R\boldsymbol{u}(\tau)\right]\, d\tau \tag{4.20}$$

subject to the dynamical constraints

$$\begin{pmatrix} I_{nd} & 0 \\ 0 & 0 \end{pmatrix}\begin{pmatrix} \dot{\boldsymbol{v}} \\ \dot{\boldsymbol{p}} \end{pmatrix} = \begin{pmatrix} A_{11} & A_{12} \\ A_{21} & 0 \end{pmatrix}\begin{pmatrix} \boldsymbol{v} \\ \boldsymbol{p} \end{pmatrix} + \begin{pmatrix} B_1 \\ B_2 \end{pmatrix}\boldsymbol{u} + \begin{pmatrix} C_1 \\ C_2 \end{pmatrix}, \tag{4.21}$$

where I_{nd} is the $nd \times nd$ identity matrix, $A_{11} \in \Re^{nd\times nd}$, $A_{12} \in \Re^{nd\times n}$, $A_{21} \in \Re^{n\times nd}$, $B_1 \in \Re^{nd\times 1}$, $B_2 \in \Re^{n\times 1}$, $C_1 \in \Re^{nd\times 1}$, $C_2 \in \Re^{n\times 1}$, n is the number of computational nodes, and d is the number of physical dimensions of the system (either 1, 2, or 3). As usual, the system Lagrangian is produced by appending the state to the cost functional using Lagrangian multiplier functions:

$$\begin{aligned} L = \int_0^\infty &\left[\boldsymbol{v}^T Q_v\boldsymbol{v} + \boldsymbol{p}^T Q_p\boldsymbol{p} + \boldsymbol{u}^T R\boldsymbol{u}\right]\, d\tau \\ &+ \int_0^\infty \boldsymbol{\psi}_v^T\left[A_{11}\boldsymbol{v} + A_{12}\boldsymbol{p} + B_1\boldsymbol{u} + C_1\right]\, d\tau \\ &+ \int_0^\infty \boldsymbol{\psi}_p^T\left[A_{21}\boldsymbol{v} + B_2\boldsymbol{u} + C_2\right]\, d\tau. \end{aligned} \tag{4.22}$$

The first variation of L is produced by taking small perturbations on $\boldsymbol{u}$:

$$\begin{aligned} \delta L = \int_0^\infty &\left[\boldsymbol{v}^T Q_v\delta\boldsymbol{v} + \boldsymbol{p}^T Q_p\delta\boldsymbol{p} + \boldsymbol{u}^T R\delta\boldsymbol{u}\right]\, d\tau \\ &+ \int_0^\infty \boldsymbol{\psi}_v^T\left[A_{11}\delta\boldsymbol{v} + A_{12}\delta\boldsymbol{p} + B_1\delta\boldsymbol{u} - \delta\dot{\boldsymbol{v}}\right]\, d\tau \\ &+ \int_0^\infty \boldsymbol{\psi}_p^T\left[A_{21}\delta\boldsymbol{v} + B_2\delta\boldsymbol{u}\right]\, d\tau = 0. \end{aligned} \tag{4.23}$$

Since the perturbations are assumed to be small the terms $\delta \boldsymbol{v}^T Q_v \delta \boldsymbol{v}$, $\delta \boldsymbol{p}^T Q_p \delta \boldsymbol{p}$, and $\delta \boldsymbol{u}^T R \delta \boldsymbol{u}$ are neglected. Rearranging and integrating by parts yields

$$\begin{aligned}\delta L = \int_0^\infty \left[\boldsymbol{v}^T Q_v + \boldsymbol{\psi}_v^T A_{11} + \boldsymbol{\psi}_p^T A_{21} + \dot{\boldsymbol{\psi}}_v^T\right] \delta \boldsymbol{v}\, d\tau \\ + \int_0^\infty \left[\boldsymbol{p}^T Q_p + \boldsymbol{\psi}_v^T A_{12}\right] \delta \boldsymbol{p}\, d\tau \\ + \int_0^\infty \left[\boldsymbol{u}^T R + \boldsymbol{\psi}_v^T B_1 + \boldsymbol{\psi}_p^T B_2\right] \delta \boldsymbol{u}\, d\tau - \boldsymbol{\psi}_v^T \delta \boldsymbol{v}\Big|_0^\infty = 0. \quad (4.24)\end{aligned}$$

Imposing $\lim_{t\to\infty} \boldsymbol{\psi}_v(t) = 0$ and considering $\delta \boldsymbol{v}(0) \equiv 0$ forces $\boldsymbol{\psi}_v^T \delta \boldsymbol{v}\big|_0^\infty = 0$. Since equation (4.24) must be true for any value of $\delta \boldsymbol{u}$ and $\delta \boldsymbol{u}$, $\delta \boldsymbol{v}$, and $\delta \boldsymbol{p}$ are assumed to be continuous then by the Fundamental Lemma of Calculus of Variations it is enough to consider the equation

$$\begin{aligned}\left[\boldsymbol{v}^T Q_v + \boldsymbol{\psi}_v^T A_{11} + \boldsymbol{\psi}_p^T A_{21} + \dot{\boldsymbol{\psi}}_v^T\right] \delta \boldsymbol{v} + \left[\boldsymbol{p}^T Q_p + \boldsymbol{\psi}_v^T A_{12}\right] \delta \boldsymbol{p} \\ + \left[\boldsymbol{u}^T R + \boldsymbol{\psi}_v^T B_1 + \boldsymbol{\psi}_p^T B_2\right] \delta \boldsymbol{u} = 0. \quad (4.25)\end{aligned}$$

To force equation (4.25) to be true for all $\delta \boldsymbol{u}$, the multipliers $\boldsymbol{\psi}$ are chosen such that

$$\boldsymbol{v}^T Q_v + \boldsymbol{\psi}_v^T + \boldsymbol{\psi}_v^T A_{11} + \boldsymbol{\psi}_p^T A_{21} + \dot{\boldsymbol{\psi}}_v^T = 0, \quad (4.26)$$

$$\boldsymbol{\psi}_v^T A_{12} + \boldsymbol{p}^T Q_p = 0, \quad (4.27)$$

$$\boldsymbol{u}^T R + \boldsymbol{\psi}_v^T B_1 + \boldsymbol{\psi}_p^T B_2 = 0. \quad (4.28)$$

Equations (4.26) and (4.27) are the costate equations. Equation (4.28) can be used to solve for $\boldsymbol{u}$ in terms of the unknown multipliers:

$$\boldsymbol{u} = -R^{-1}\left(B_1^T \boldsymbol{\psi}_v + B_2^T \boldsymbol{\psi}_p\right). \quad (4.29)$$

Substituting eq. (4.29)into eq. (4.21), the state-costate system is

$$\begin{pmatrix} I & 0 & 0 & 0 \\ 0 & -I & 0 & 0 \\ 0 & 0 & 0 & 0 \\ 0 & 0 & 0 & 0 \end{pmatrix} \begin{pmatrix} \dot{\boldsymbol{v}} \\ \dot{\boldsymbol{\psi}}_v \\ \dot{\boldsymbol{p}} \\ \dot{\boldsymbol{\psi}}_p \end{pmatrix} = \begin{pmatrix} A_{11} & -B_1R^{-1}B_1^T & A_{12} & -B_1R^{-1}B_2^T \\ Q_v & A_{11}^T & 0 & A_{21}^T \\ A_{21} & -B_2R^{-1}B_1^T & 0 & -B_2R^{-1}B_2^T \\ 0 & A_{12}^T & Q_p & 0 \end{pmatrix} \begin{pmatrix} \boldsymbol{v} \\ \boldsymbol{\psi}_v \\ \boldsymbol{p} \\ \boldsymbol{\psi}_p \end{pmatrix} + \begin{pmatrix} C_1 \\ 0 \\ C_2 \\ 0 \end{pmatrix}. \quad (4.30)$$

4.2.4 Continuous-Time Algebraic Riccati Equation for the Discretized Navier-Stokes Equations: The General Case

Assume that the Lagrangian multipliers take the form $\boldsymbol{\psi}_v = P_1\boldsymbol{v} + \boldsymbol{k}_1$, $\boldsymbol{\psi}_p = P_2\boldsymbol{p} + \boldsymbol{k}_1$. Then the system (4.30) becomes

$$\begin{aligned} \dot{\boldsymbol{v}} = A_{11}\boldsymbol{v} + A_{12}\boldsymbol{p} - B_1R^{-1}B_1^TP_1\boldsymbol{v} - B_1R^{-1}B_1^T\boldsymbol{k}_1 \\ -B_1R^{-1}B_2^TP_2\boldsymbol{p} - B_1R^{-1}B_2^T\boldsymbol{k}_2 + C_1, \end{aligned} \quad (4.31)$$

$$0 = Q_v\boldsymbol{v} + A_{11}^TP_1\boldsymbol{v} + A_{11}^T\boldsymbol{k}_1 + A_{21}^TP_2\boldsymbol{p} + A_{21}^T\boldsymbol{k}_2 + P_1\dot{\boldsymbol{v}}, \quad (4.32)$$

$$\begin{aligned} 0 = A_{21}\boldsymbol{v} - B_2R^{-1}B_1^TP_1\boldsymbol{v} - B_2R^{-1}B_1^T\boldsymbol{k}_1 \\ -B_2R^{-1}B_2^TP_2\boldsymbol{p} - B_2R^{-1}B_2^T\boldsymbol{k}_2 + C_2, \end{aligned} \quad (4.33)$$

$$0 = A_{12}^TP_1\boldsymbol{v} + A_{12}^T\boldsymbol{k}_1 + Q_p\boldsymbol{p}. \quad (4.34)$$

Substituting eq. (4.31) into eq. (4.32):

$$\begin{aligned} Q_v\boldsymbol{v} + A_{11}^TP_1\boldsymbol{v} + A_{11}^T\boldsymbol{k}_1 + A_{21}^TP_2\boldsymbol{p} + A_{21}^T\boldsymbol{k}_2 \\ + P_1\big(A_{11}\boldsymbol{v} + A_{12}\boldsymbol{p} - B_1R^{-1}B_1^TP_1\boldsymbol{v} - B_1R^{-1}B_1^T\boldsymbol{k}_1 \\ -B_1R^{-1}B_2^TP_2\boldsymbol{p} - B_1R^{-1}B_2^T\boldsymbol{k}_2 + C_1\big) = 0. \end{aligned} \quad (4.35)$$

The state-costate system now consists of equations (4.33), (4.34), and (4.35). For analysis, eq. (4.33) is pre-multiplied by P_2 and add it to eq. (4.34). The full state-costate system in

matrix form:

$$\begin{pmatrix} Q_v & 0 \\ 0 & Q_p \end{pmatrix}\begin{pmatrix} \boldsymbol{v} \\ \boldsymbol{p} \end{pmatrix} + \begin{pmatrix} A_{11}^T & A_{21}^T \\ A_{12}^T & 0 \end{pmatrix}\begin{pmatrix} P_1 & 0 \\ 0 & P_2 \end{pmatrix}\begin{pmatrix} \boldsymbol{v} \\ \boldsymbol{p} \end{pmatrix} + \begin{pmatrix} A_{11}^T & A_{21}^T \\ A_{12}^T & 0 \end{pmatrix}\begin{pmatrix} \boldsymbol{k}_1 \\ \boldsymbol{k}_2 \end{pmatrix}$$
$$+ \begin{pmatrix} P_1 & 0 \\ 0 & P_2 \end{pmatrix}\begin{pmatrix} A_{11} & A_{12} \\ A_{21} & 0 \end{pmatrix}\begin{pmatrix} \boldsymbol{v} \\ \boldsymbol{p} \end{pmatrix}$$
$$- \begin{pmatrix} P_1 & 0 \\ 0 & P_2 \end{pmatrix}\begin{pmatrix} B_1R^{-1}B_1^T & B_1R^{-1}B_2^T \\ B_2R^{-1}B_1^T & B_2R^{-1}B_2^T \end{pmatrix}\begin{pmatrix} P_1 & 0 \\ 0 & P_2 \end{pmatrix}\begin{pmatrix} \boldsymbol{v} \\ \boldsymbol{p} \end{pmatrix}$$
$$- \begin{pmatrix} P_1 & 0 \\ 0 & P_2 \end{pmatrix}\begin{pmatrix} B_1R^{-1}B_1^T & B_1R^{-1}B_2^T \\ B_2R^{-1}B_1^T & B_2R^{-1}B_2^T \end{pmatrix}\begin{pmatrix} \boldsymbol{k}_1 \\ \boldsymbol{k}_2 \end{pmatrix} + \begin{pmatrix} P_1 & 0 \\ 0 & P_2 \end{pmatrix}\begin{pmatrix} C_1 \\ C_2 \end{pmatrix} = 0. \quad (4.36)$$

Equation (4.36) takes on the familiar form of eq. (4.18). Ideally, we would like to reduce eq. (4.36) to a system similar to eqs. (4.13) and (4.14) but there are two obstacles preventing this:

1. Solving eqs. (4.13) and (4.14) does not guarantee that either of conditions (4.33) or (4.34) are met.

2. Solving eqs. (4.13) and (4.14) does not guarantee that the solution matrix takes the form
$$P = \begin{pmatrix} P_1 & 0 \\ 0 & P_2 \end{pmatrix}. \quad (4.37)$$

Furthermore, recall that eq. (4.18) reduces to eqs. (4.13) and (4.14) on condition that eq. (4.18) holds for all $\boldsymbol{x} \in \Re^n$. If a solution does exist for eq. (4.18) for all $\boldsymbol{x} \in \Re^n$ then the solution also satisfies eq. (4.18) for all $\boldsymbol{x}$ in any vector space which is a subset of $\Re^n$, and hence the solution to the system (4.13), (4.14) also satisfies eq. (4.18), regardless of the restrictions on $\boldsymbol{x}$. However, the restriction $x \in \Re^n$ is overly restrictive and there may not actually exist a solution to the system (4.13), (4.14) that has the form (4.37). Rather, solutions of the form (4.37) may only exist when the domain of x is restricted to the solution space of eq. (4.33).

Let $S = \{\mathbf{v} \in \Re^{\mathbf{n}},\ \mathbf{v} \text{ satisfies eq. (4.33)}\}$. If a map can be constructed $M : \mathbf{w} \to \mathbf{v}$ for all $\mathbf{w} \in \Re^{\mathbf{m}}$ and $\mathbf{v} \in S$, $m < n$, then the system (4.36) can be written in terms of $\boldsymbol{w}$ and $\boldsymbol{p}$. This would ultimately allow eq. (4.36) to be written independently of the state variables. Also, eq. (4.33) would now be implicit to the system and hence solving eq. (4.36) would ensure both conditions (4.33) and (4.34). However, it is not clear how to construct

this mapping in the general case since eq. (4.33) is a complicated function including $\boldsymbol{p}$, $\boldsymbol{k}_1$, and $\boldsymbol{k}_2$. Section 4.2.5 will demonstrate a special case where such a mapping can easily be constructed.

4.2.5 Continuous-Time Algebraic Riccati Equation for the Discretized Navier-Stokes Equations when $B_2 = 0$, $C_1 = 0$, and $C_2 = 0$

In this special case, we will assume that $\boldsymbol{\psi}_v = P_1\boldsymbol{v}$ and will with-hold any assumptions on $\boldsymbol{\psi}_p$ for the moment. The state-costate equations (4.31)-(4.34) under this assumption are written as:

$$\dot{\boldsymbol{v}} = A_{11}\boldsymbol{v} + A_{12}\boldsymbol{p} - B_1R^{-1}B_1^TP_1\boldsymbol{v}, \tag{4.38}$$

$$0 = Q_v\boldsymbol{v} + A_{11}^TP_1\boldsymbol{v} + A_{21}^T\boldsymbol{\psi}_p + P_1\dot{\boldsymbol{v}}, \tag{4.39}$$

$$0 = A_{21}\boldsymbol{v}, \tag{4.40}$$

$$0 = A_{12}^TP_1\boldsymbol{v} + Q_p\boldsymbol{p}. \tag{4.41}$$

Pre-multiplying eq. (4.38) by A_{21}:

$$A_{21}\dot{\boldsymbol{v}} = A_{21}A_{11}\boldsymbol{v} + A_{21}A_{12}\boldsymbol{p} - A_{21}B_1R^{-1}B_1^TP_1\boldsymbol{v}. \tag{4.42}$$

From eq. (4.40), $A_{21}\boldsymbol{v} = 0 \Rightarrow A_{21}\dot{\boldsymbol{v}} = 0$. Hence:

$$A_{21}A_{11}\boldsymbol{v} + A_{21}A_{12}\boldsymbol{p} - A_{21}B_1R^{-1}B_1^TP_1\boldsymbol{v} = 0. \tag{4.43}$$

From this,

$$\boldsymbol{p} = \left(A_{21}A_{12}\right)^{-1}\left[A_{21}B_1R^{-1}B_1^TP_1 - A_{21}A_{11}\right]\boldsymbol{v}. \tag{4.44}$$

Of course in eq. (4.44) it has been assumed that $A_{21}A_{12}$ is invertible. To investigate whether this is justifiable, the finite element case is analyzed.

Let $\tilde{A}_{21}$ and $\tilde{A}_{12}$ be the finite element versions of A_{21} and A_{12} respectively. Matrix $\tilde{A}_{21}$ corresponds to the term $\nabla \cdot \boldsymbol{v}$ in the mass equation (4.1) and $\tilde{A}_{12}$ corresponds to the term $\nabla\boldsymbol{p}$ in the momentum equation (4.2). Since ∇ and $\nabla\cdot$ are adjoint operators, the finite element discretization leads to the property $\tilde{A}_{12} = \tilde{A}_{21}^T$. Hence, $\tilde{A}_{21}\tilde{A}_{12} = \tilde{A}_{21}\tilde{A}_{21}^T$.

Let n be the number of control volumes and let d be the dimension of the system. By construction, $\tilde{A}_{21} \in \Re^{n\times dn}$ and $\tilde{A}_{21}^T \in \Re^{dn\times n}$. Assume that $rank\left(\tilde{A}_{21}\right) = rank\left(\tilde{A}_{21}^T\right) =$

n since if $\tilde{A}_{21}$ was not full rank then the numerical fluid flow problem would not be uniquely solveable. Furthermore, define the subspace

$$\tilde{S} = \left\{ \boldsymbol{v} \in \Re^{dn}, \quad \boldsymbol{v} \in ker\left(\tilde{A}_{21}\right) \right\}, \tag{4.45}$$

taking note that $dim(\tilde{S}) = n\,(d-1)$. Since each column of $\tilde{A}_{21}^T$ is parallel to a row of $\tilde{A}_{21}$, then the column space of A_{21}^T is not in $\tilde{S}$. Since the column space of $\tilde{A}_{21}^T$ consists of n linearly independent vectors then the column space of $\tilde{A}_{21}^T$ forms a basis for the orthogonal complement of $\tilde{S}$, defined

$$\tilde{S}^c = \left\{ \boldsymbol{v} \in \Re^{dn}, \quad \boldsymbol{v} \notin ker\left(\tilde{A}_{21}\right) \right\}. \tag{4.46}$$

Hence, $rank\left(\tilde{A}_{21}\right) = dim\left(image\left(\tilde{A}_{21}\right)\right) = rank\left(\tilde{A}_{21}\tilde{A}_{21}^T\right) = n$. Since $\tilde{A}_{21}\tilde{A}_{21}^T \in \Re^{n\times n}$ and $rank\left(\tilde{A}_{21}\tilde{A}_{21}^T\right) = n$, then $\tilde{A}_{21}\tilde{A}_{21}^T$ is invertible.

Similarly, construct

$$S = \left\{ \boldsymbol{v} \in \Re^{dn}, \quad \boldsymbol{v} \in ker\left(A_{21}\right) \right\}, \tag{4.47}$$

$$S^c = \left\{ \boldsymbol{v} \in \Re^{dn}, \quad \boldsymbol{v} \notin ker\left(A_{21}\right) \right\} \tag{4.48}$$

for the finite volume discretization. Discretizing by the finite volume method requires consideration of the governing equations in their weak (conservation) form. The pressure term from the momentum is discretized over a control volume of volume $\forbidden{V}$:

$$\iiint_{\forbidden{V}_i} \nabla \boldsymbol{p}_i \, d\forbidden{V}_i \rightarrow \forbidden{V}_i \nabla \boldsymbol{p}_i, \tag{4.49}$$

and $\nabla \boldsymbol{p}_i$ is discretized by finite differences. Hence, the columns of A_{12} are parallel to the columns of $\tilde{A}_{12}$. However, the discretization for the conservation of mass equation for the finite-volume method over a control volume is

$$\iiint_{\forbidden{V}_i} \nabla \cdot \boldsymbol{v} \, d\forbidden{V}_i = \iint_{A_r} \boldsymbol{v} \cdot \hat{\boldsymbol{n}} \, dA^s \rightarrow \sum_{i=1}^{\#\text{faces}} A_i^s \boldsymbol{v} \cdot \hat{\boldsymbol{n}}_i, \tag{4.50}$$

where A^s is the area of a control volume face and $\hat{\boldsymbol{n}}$ is the unit vector normal to the surface of the control volume. Equation (4.50) does not take the same form as the finite element formulation. However, since the solution to the dynamical system is expected to

be (approximately) independent of the discretization method, then by consistency of the conservation of mass equation

$$ker\left(A_{21}\right) = ker\left(\tilde{A}_{21}\right). \tag{4.51}$$

Hence, $S = \tilde{S}$ and $S^c = \tilde{S}^c$. Since the columns of A_{12} span $\tilde{S}^c$ and $S^c = \tilde{S}^c$, then the columns of A_{12} span S^c and hence $A_{21}A_{12}$ is invertible. This can also be verified numerically since the assumption (4.51) will only be approximate in practice.

Substituting eq. (4.38) into eq. (4.39):

$$Q_v\boldsymbol{v} + A_{11}^T P_1\boldsymbol{v} + A_{21}^T\boldsymbol{\psi}_2 + P_1A_{11}\boldsymbol{v} + P_1\left(A_{11}\boldsymbol{v} + A_{12}\boldsymbol{p} - B_1R^{-1}B_1^TP_1\boldsymbol{v}\right) = 0. \tag{4.52}$$

Now, substituting eq. (4.43) into eq. (4.52):

$$Q_v\boldsymbol{v} + A_{11}^T P_1\boldsymbol{v} + A_{21}^T\boldsymbol{\psi}_2 + P_1A_{11}\boldsymbol{v} + P_1A_{12}\left(A_{21}A_{12}\right)\left[A_{21}B_1R^{-1}B_1^TP_1 - A_{21}A_{11}\right] - P_1B_1R^{-1}B_1^TP_1\boldsymbol{v} = 0. \tag{4.53}$$

Finally, substitute eq. (4.43) into eq. (4.41):

$$A_{21}^T P_1\boldsymbol{v} + Q_p\left(A_{21}A_{12}\right)^{-1}\left[A_{21}B_1R^{-1}B_1^TP_1 - A_{21}A_{11}\right]\boldsymbol{v} = 0. \tag{4.54}$$

The solution to the linear quadratic regulator problem is

$$\boldsymbol{u} = -R^{-1}\left(B_1^TP_1\boldsymbol{v}\right), \tag{4.55}$$

where P_1 is determined implicitly by eqs. (4.53), (4.54) and (4.40). The multipliers $\boldsymbol{\psi}_p$ are not explicit in eq. (4.55) but it is a requirement that they exist. This problem can be interpreted as solving eqs. (4.53) and (4.54) where $\boldsymbol{v}$ is restricted to the subspace S defined in (4.47). If $[\boldsymbol{s}_i]$ is an orthonormal basis for S then there exist $w_i \in \Re$ such that $\boldsymbol{v} = \sum w_i\boldsymbol{s}_i$ for all $\boldsymbol{v} \in S$. Defining S_v as the matrix whose columns are the ordered basis vectors $\boldsymbol{s}_i$, this can alternatively be written as $\boldsymbol{v} = S_v\boldsymbol{w}$, where $\boldsymbol{w}$ contains w_i in the appropriate order. Define:

$$W = \left\{\boldsymbol{w} \in \Re^n, \quad V\boldsymbol{w} \in S\right\}. \tag{4.56}$$

Since there exists $\boldsymbol{w}$ for all $\boldsymbol{v} \in S$ such that $\boldsymbol{v} = S_v\boldsymbol{w}$ and $dim(S) = n$, then $dim(W) = n$. Hence $W = \Re^n$. Furthermore, we will now look for a solution where $\boldsymbol{\psi}_p = P_2\boldsymbol{w}$.

Now, substitute $\boldsymbol{v} = S_v \boldsymbol{w}$ and $\boldsymbol{\psi}_p = P_2 \boldsymbol{w}$ into eqs. (4.53) and (4.54):

$$Q_v S_v \boldsymbol{w} + A_{11}^T P_1 S_v \boldsymbol{w} + A_{21}^T P_2 \boldsymbol{w} + P_1 A_{11} S_v \boldsymbol{w} + P_1 A_{12} \left(A_{21} A_{12}\right)^{-1} \left[A_{21} B_1 R^{-1} B_1^T P_1 - A_{21} A_{11}\right] S_v \boldsymbol{w} - P_1 B_1 R^{-1} B_1^T P_1 S_v \boldsymbol{w} = 0, \quad (4.57)$$

$$A_{12}^T P_1 S_v \boldsymbol{w} + Q_p \left(A_{21} A_{12}\right)^{-1} \left[A_{21} B_1 R^{-1} B_1^T P_1 - A_{21} A_{11}\right] S_v \boldsymbol{w} = 0. \quad (4.58)$$

These equations take the form $M\boldsymbol{w} = 0$. If $M\boldsymbol{w} = 0$ for all $\boldsymbol{w} \in \Re^n$, then $M = 0$. Hence:

$$Q_v S_v + A_{11}^T P_1 S_v + A_{21}^T P_2 + P_1 A_{11} S_v + P_1 A_{12} \left(A_{21} A_{12}\right)^{-1} \left[A_{21} B_1 R^{-1} B_1^T P_1 - A_{21} A_{11}\right] S_v - P_1 B_1 R^{-1} B_1^T P_1 S_v = 0, \quad (4.59)$$

$$A_{12}^T P_1 S_v + Q_p \left(A_{21} A_{12}\right)^{-1} \left[A_{21} B_1 R^{-1} B_1^T P_1 - A_{21} A_{11}\right] S_v = 0. \quad (4.60)$$

Equations (4.59) and (4.60) are second order non-linear matrix algebraic equations which cannot be solved by analytical means. Numerical solutions may be possible but are not easily obtained. However, if the solution to these equations is approximated by some other method then these equations can be used to investigate the validity of the solution.

4.2.6 Minimum-Norm Solution

Consider once more the problem of solving eqs. (4.53) and (4.54) where $\boldsymbol{v}$ is restricted to S and assume that there exists $\boldsymbol{\psi}_p^*$ such that P_1^* solves this system. Since $v \notin S$ is not being considered, the control $\boldsymbol{u}$ may be arbitrary when $\boldsymbol{v} \notin S$ and hence the mapping $P_1^* \boldsymbol{s}^c$, where $\boldsymbol{s}^c$ is the component of $\boldsymbol{v}$ in S^c, is arbitrary as well. Hence, P_1^* will not be unique.

Naturally, two questions arise from this observation:

1. Does it matter which specific solution is chosen?

2. If a particular solution is desired, how can it be constructed?

Consider that the feedback law for this problem is generated from a particular linearization of the state equations and as the system evolves, the system dynamics will not satisfy the

original linearization. Even in the fully linear case, one cannot expect to have $\boldsymbol{v} \in S$ exactly, due to numerical or especially experimental error and there is no assurance that the mapping of P_1^* on any component of $\boldsymbol{v}$ not in S (which takes the form $P_1^* \boldsymbol{s}^c$, $\boldsymbol{s}^c \in S^c$) will be small (even if $\|\boldsymbol{s}^c\|$ is small). Any vector $\boldsymbol{v} \in \Re^{dn}$ can be written $\boldsymbol{v} = \boldsymbol{s} + \boldsymbol{s}^c$, where $\boldsymbol{s}$ and $\boldsymbol{s}^c$ are linear combinations of the basis vectors $\boldsymbol{s}_i$ and $\boldsymbol{s}_i^c$ respectively. Since the quantity $P_1^* \boldsymbol{s}^c$ is arbitrary and has no physical meaning, the best strategy is to eliminate this component is by constructing the particular solution, denoted $P_1^\#$, as follows:

$$P_1^\# \boldsymbol{s} = P_1^* \boldsymbol{s}, \tag{4.61}$$

$$P_1^\# \boldsymbol{s}^c = 0. \tag{4.62}$$

The result of such a construction is

$$P_1^\# \boldsymbol{v} = P_1^\# (\boldsymbol{s} + \boldsymbol{s}^c) = P_1^* \boldsymbol{s}. \tag{4.63}$$

The particular solution was constructed in this way in Stoyanov (2006) for the finite element case and the same construction will work here. The algebraic construction

$$P_1^\# = P_1^* S_v S_v^T \tag{4.64}$$

where the columns of S_v are an orthonormal basis for S (as defined earlier) was shown in Stoyanov (2006) to be the appropriate construction in the finite element case and so it is investigated here as the construction satisfying conditions (4.63) for the finite volume case as well.

There are two important properties of the matrix S_v:

1. $S_v^T S_v = I$,
2. $S_v \boldsymbol{v}_1 = S_v \boldsymbol{v}_2 \Rightarrow \boldsymbol{v}_1 = \boldsymbol{v}_2$ for all $\boldsymbol{v} \in \Re^{dn}$.

It follows that if $\boldsymbol{b} = S_v S_v^T \boldsymbol{s}$ for some $\boldsymbol{s} \in S$ and $\boldsymbol{b} \in \Re^n$, then Property 1 gives $S_v^T \boldsymbol{b} = S_v^T \boldsymbol{s}$, which by Property 2 gives $\boldsymbol{b} = \boldsymbol{s}$. Hence, condition (4.61) is satisfied. Also, since $\boldsymbol{s}^c$ is orthogonal to the rows of S_v^T, then $S_v^T \boldsymbol{s}^c = 0$ and hence condition (4.62) is satisfied. Hence eq. (4.64) is the appropriate construction to satisfy eq. (4.63).

4.2.7 Perturbation Methods

Consider a linear dynamical system of the form

$$\begin{pmatrix} I_m & 0 \\ 0 & 0 \end{pmatrix} \begin{pmatrix} \dot{v}(t) \\ \dot{p}(t) \end{pmatrix} = \begin{pmatrix} A_{11} & A_{12} \\ A_{21} & A_{22} \end{pmatrix} \begin{pmatrix} v(t) \\ p(t) \end{pmatrix} + \begin{pmatrix} B_1 \\ B_2 \end{pmatrix} u(t) + \begin{pmatrix} C_1 \\ C_2 \end{pmatrix}, \quad (4.65)$$

where I_m is the $m \times m$ identity matrix, $A_{11} \in \Re^{m \times m}$, $A_{12} \in \Re^{m \times n}$, $A_{21} \in \Re^{n \times m}$, $B_1 \in \Re^{m \times 1}$, $B_2 \in \Re^{n \times 1}$, $C_1 \in \Re^{m \times 1}$, $C_2 \in \Re^{n \times 1}$. This system of equations has a differential part and an algebraic part:

$$\dot{\mathbf{v}}(t) = A_{11}\mathbf{v}(t) + A_{12}\mathbf{p}(t) + B_1\mathbf{u}(t) + C_1, \quad (4.66)$$

$$\mathbf{0} = A_{21}\mathbf{v}(t) + A_{22}\mathbf{p}(t) + B_2\mathbf{u}(t) + C_2. \quad (4.67)$$

If A_{22} is invertible then it is possible to solve for $\mathbf{p}(t)$ from eq. (4.67):

$$\mathbf{p}(t) = -A_{22}^{-1}\left(A_{21}\mathbf{v}(t) + B_2\mathbf{u}(t) + C_2\right). \quad (4.68)$$

Substitution into eq. (4.66) gives:

$$\dot{\mathbf{v}}(t) = A_0\mathbf{v}(t) + B_0\mathbf{u}(t) + C_0, \quad (4.69)$$

where $A_0 = A_{11} - A_{12}A_{22}^{-1}A_{21}$, $B_0 = B_1 - A_{12}A_{22}^{-1}B_2$, and $C_0 = C_1 - A_{12}A_{22}^{-1}C_2$. Of course, a critical feature of the discretized Navier-Stokes equations is that A_{22} is singular. In fact, it is the zero matrix. However, an invertible matrix can be created artificially by setting, for example, $A_{22} = \varepsilon I_n$, where ε is small. The feedback law is generated for this modified control system by eqs. (4.12-4.14) and is denoted $\mathbf{u}_0(\mathbf{v})$.

In Stoyanov (2006), the special case $B_2 = 0$, $C_1 = 0$, $C_2 = 0$, $Q_p = 0$ is considered. In this case, the author shows that if the perturbation method converges (in the sense that the solution to the corresponding Riccati equation exists as the norm of A_{22} becomes arbitrarily small), then the solution P_0 of the Riccati equation for the perturbed system also satisfies the Riccati equations for the unperturbed system. However, the condition $A_{12}^T = A_{21}$ is an important feature of this proof and it would be necessary to at least show that $ker(A_{12}^T) = ker(A_{21})$ to construct a proof by the same method, which is not justifiable for the finite volume method. Alternatively, the perturbation method will be used in Section 4.3 of this paper and the solution will be verified numerically as the solution to eqs. (4.59) and (4.60).

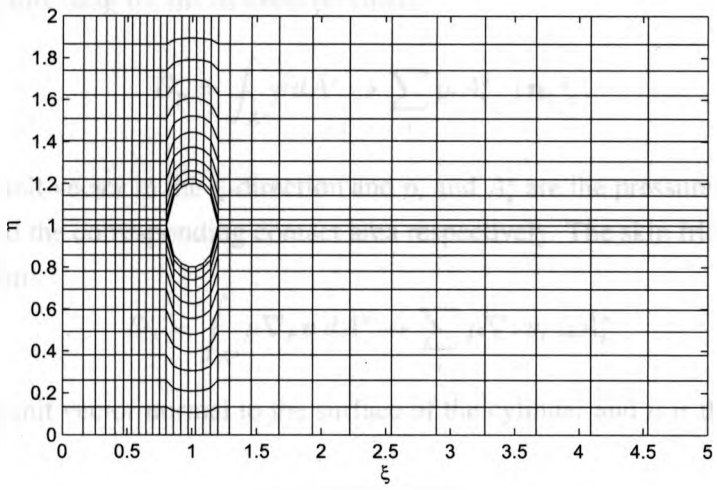

Figure 4.1: Mesh generation for channel flow across a cylinder with 660 control volumes.

4.3 Drag Minimization in a Channel Around a Cylindrical Obstruction

The control problem was formulated and solved for a two-dimensional fluid flow system. The simulation provided some insight into the nature of the problem and emphasized some important considerations.

4.3.1 Problem Formulation

The system for analysis is depicted in Figure 4.1 and was coded in Matlab. Dirichlet boundary condition was used to specify a constant velocity profile at the west edge of the domain. The north and south edges of the domain and the surface of the cylinder were treated as walls with no slip condition ($\mathbf{v} = 0$). Neuman condition $\left(\frac{\partial \mathbf{v}}{\partial \xi} = 0\right)$ was applied to the velocity profile at the east face, where ξ is the lateral spacial variable as indicated in Figure 4.1. The condition $P = 0$ was also set at the east face. The system was solved on a block-structured grid using a change of coordinate method (Liseikin, 1999; Thompson et al, 1985). The control mechanism is the angular velocity of the cylinder.

The control problem is formulated as the minimization of the drag across the cylinder subject to the constraints provided by the system dynamics, which are given by eqs. (4.1)-

(4.2). The pressure drag for the discrete problem:

$$D_p = \int_{A^s} p\, dA^s \rightarrow \sum_i p_i A_i^s \cdot (\hat{\boldsymbol{n}}_\xi)_i\,, \tag{4.70}$$

where $\hat{\boldsymbol{n}}_\xi$ is a unit vector in the $\boldsymbol{\xi}$-direction and p_i and A_i^s are the pressure at the surface of the cylinder and the corresponding contact area respectively. The skin friction drag for the discrete problem:

$$D_s = \int_{A^s} \mu \nabla_{\hat{\boldsymbol{r}}} \boldsymbol{v}\, dA^s \rightarrow \sum_i \mu \nabla_{\hat{\boldsymbol{r}}} \boldsymbol{v}_i\, \Delta A_i^s, \tag{4.71}$$

where $\hat{\boldsymbol{r}}$ is the unit vector normal to the surface of the cylinder and μ is the viscosity. The total drag:

$$D_t = D_p + D_s. \tag{4.72}$$

The cost functional needs to be written in a form amenable to the solution strategy of section 4.2.2. Since equation (4.72) is linear it can be written in the form:

$$D_p = \begin{pmatrix} q_v & q_p \end{pmatrix} \begin{pmatrix} \mathbf{v} \\ \mathbf{p} \end{pmatrix} = 0. \tag{4.73}$$

Finally, the cost functional is written in terms of D_t^2:

$$J = \int_0^\infty \mathbf{x}^T Q \mathbf{x} + u^T R u\, dt, \quad Q = \begin{pmatrix} q_v^T \\ q_p^T \end{pmatrix} \begin{pmatrix} q_v & q_p \end{pmatrix}, \quad \mathbf{x} = \begin{pmatrix} \mathbf{v} \\ \mathbf{p} \end{pmatrix},$$
$$R \in \Re,\ R > 0. \tag{4.74}$$

Since $D_t^2 \geq 0$, then $\mathbf{x}^T Q \mathbf{x} \geq 0\ \forall \mathbf{x}$. This, paired with $R > 0$, ensures well-posedness for the control problem.

4.3.2 Linearization

The choice of linearization point is fundamental to this problem. From the Navier-stokes equations (4.1)-(4.2) the only nonlinearity is the term $\mathbf{v} \cdot \nabla \mathbf{v}$. This term may be linearized

about the origin, resulting in the linearized momentum equations:

$$\rho\frac{\partial \mathbf{v}}{\partial t} + \nabla p = \mu\nabla^2\mathbf{v}. \tag{4.75}$$

The flow may alternatively be linearized about a non-zero velocity field. The momentum equations in this case:

$$\rho\left(\frac{\partial \mathbf{v}}{\partial t} + \bar{\mathbf{V}}\cdot\nabla\mathbf{v}\right) + \nabla p = \mu\nabla^2\mathbf{v}, \tag{4.76}$$

where $\bar{\mathbf{V}}$ is a lagged velocity term. Since the final flow field will not be known a priori a suitable choice of $\bar{\mathbf{V}}$ might be the initial state.

Equations (4.75) and (4.76) are known as the Stokes and Oseen equations respectively. Since equation (4.76) is linearized closer to the current state it will generally be more accurate to use this linearization. The advantage to the Stokes method is that the Dirichlet boundary conditions on the west face $\mathbf{v}(\xi=0,t) = \mathbf{v}_0(t)$ is replaced with $\mathbf{v}(\xi=0,t) = 0$, the effect being a purely homogeneous linearization.

4.3.3 Convergence of the Perturbation Method

Since the control law does not contribute to the conservation of mass equation the condition $B_2 = 0$ is automatically met. The Stokes linearization (4.75) was employed to satisfy conditions $C_1 = 0$, $C_2 = 0$. Furthermore, the condition $Q_p = 0$ was imposed by considering only the skin friction drag in the cost functional.

The perturbed system was generated by setting $A_{22} = \varepsilon I_n$ and the solution P_0 to the Riccati equation of the perturbed system was produced using the *lqr* command in Matlab. The matrix P_0 is a very large matrix so only the first few elements are produced here for several values of ε. To demonstrate convergence it is sufficient to consider a coarse grid with only 130 control volumes. Some numerical values are displayed in Table 4.3.3, from which it is apparent that the method converges in the limit $\varepsilon \to 0$.

The *lqr* algorithm in Matlab is not designed for large sparse systems, and as such some numerical difficulties are encountered when a larger number of control volumes is used. Generally, when ε is small enough the algorithm will begin to give a warning message warning that the solution may be inaccurate. When ε is made smaller still the *lqr* algorithm will cease to converge. This effect is observed clearly when 216 control volumes are used. In this case, the warning message begins to appear at about $\varepsilon = -5\times10^{-5}$. Table 4.2 shows that there is clearly some agreement between the values for each ε but no clear

		Index of P_0					
		$(1,1)$	$(1,2)$	$(1,3)$	$(1,4)$	$(1,5)$	$(1,6)$
ε	-1E-4	2.163E-13	1.537E-12	1.604E-12	3.082E-12	3.239E-12	3.557E-12
	-1E-5	2.196E-13	1.562E-12	1.628E-12	3.119E-12	3.290E-12	3.594E-12
	-1E-6	2.205E-13	1.565E-12	1.630E-12	3.123E-12	3.294E-12	3.597E-12
	-1E-7	2.204E-13	1.563E-12	1.629E-12	3.123E-12	3.295E-12	3.597E-12

Table 4.1: Some elements of P_0 for the rotating cylinder control problem for several values of ε with 130 control volumes and $Q_p = 0$.

		Index of P_0					
		$(1,1)$	$(1,2)$	$(1,3)$	$(1,4)$	$(1,5)$	$(1,6)$
ε	-5E-3	2.042E-13	3.300E-13	5.428E-13	7.152E-13	9.163E-13	1.219E-12
	-2E-3	2.260E-13	3.313E-13	5.786E-13	7.219E-13	9.633E-13	1.230E-12
	-1E-3	2.270E-13	3.271E-13	5.751E-13	7.089E-13	9.698E-13	1.211E-12
	-5E-4	2.395E-13	3.390E-13	6.182E-13	7.206E-13	9.791E-13	1.202E-12
	-2E-4	2.521E-13	3.923E-13	6.289E-13	7.124E-13	9.425E-13	1.160E-12
	-1E-4	2.458E-13	3.914E-13	5.594E-13	6.781E-13	9.022E-13	1.148E-12
	-5E-5	1.021E-13	7.712E-14	3.601E-13	5.371E-13	8.199E-13	1.095E-12
	-2E-5	1.751E-13	2.711E-13	5.913E-13	7.300E-13	1.019E-12	1.186E-12

Table 4.2: Some elements of P_0 for the rotating cylinder control problem for several values of ε with 216 control volumes and $Q_p = 0$.

convergence pattern is observed.

To verify that the solution of the perturbed system also satisfies the Riccati equations for the unperturbed system, $P_0^{\#} = P_0 S_v S_v^T$ was substituted into eq. (4.60) and the residuals were calculated. The residuals were calculated using the induced norms $\|\cdot\|_1$, $\|\cdot\|_2$, and $\|\cdot\|_\infty$, as well as the Frobenius norm. To gauge the relative magnitude of these values, the residuals were also produced for $P_1 = P_r^{\#}$, where $P_r^{\#} = P_r S_v S_v^T$ and P_r is an arbitrary matrix with the properties $P_r = P_r^T$ and $\|P_r\|_2 = \|P_0\|_2$. The data is presented in Table 4.3.3 and indicates that P_0 is a solution to eq. (4.60).

Though the matrix P_2 is redundant in this case, it is a necessary condition that such a matrix exists that satisfies eq. (4.59). To verify this, eq. (4.59) was solved numerically for P_2 in the least squares sense for both cases $P_1 = P_0^{\#}$ and $P_1 = P_r^{\#}$. The residuals from substituting the solution for P_2 back into eq. (4.59) are displayed in Table 4.3.3.

Though the residuals for eq. (4.59) are smaller with $P_0^{\#}$ than they are with $P_r^{\#}$, the difference is less than an order of magnitude. Since the least squares solution was used to determine P_2 it is not unreasonable that the residuals in both cases should be small.

Norm	$P_1 = P_0^{\#}$	$P_1 = P_r^{\#}$
$\|\cdot\|_1$	1.342E-9	1.000E-3
$\|\cdot\|_2$	3.583E-10	3.003E-4
$\|\cdot\|_\infty$	6.813E-10	1.000E-3
Frobenius	3.590E-10	3.004E-4

Table 4.3: Residuals for eq. (4.60) for the rotating cylinder control problem with $\varepsilon = -1 \times 10^{-6}$, $Q_p = 0$, and 130 control volumes.

Norm	$P_1 = P_0^{\#}$	$P_1 = P_r^{\#}$
$\|\cdot\|_1$	4.634E-5	2.532E-4
$\|\cdot\|_2$	1.988E-5	8.546E-5
$\|\cdot\|_\infty$	3.760E-5	8.546E-5
Frobenius	1.996E-5	8.650E-5

Table 4.4: Residuals for eq. (4.59) for the rotating cylinder control problem with $\varepsilon = -1 \times 10^{-6}$, $Q_p = 0$, and 130 control volumes.

However, since the residuals for $P_0^{\#}$ are smaller than the residuals for $P_r^{\#}$ but only by a relatively small margin the results should be regarded as inconclusive.

Convergence was also investigated for the case where the pressure drag is included in the cost functional but the viscous drag is neglected. This will induce $Q_v = 0$, $Q_p \neq 0$. Since $p(t)$ is not included in the perturbed cost functional, eq. (4.68) is used to write it in terms of the velocity vector $v(t)$. The cost functional for the perturbed system ultimately takes the form:

$$J = \frac{1}{2}\int_0^\infty v^T Q_0 v + 2v^T N_0 u + u^T R u \, dt, \tag{4.77}$$

$$Q_0 = A_{21}^T \left(A_{22}^{-1}\right)^T q_p^T q_p A_{22}^{-1} A_{21},$$

$$N_0 = A_{21}^T \left(A_{22}^{-1}\right)^T q_p^T q_p A_{22}^{-1} B_2,$$

$$R_0 = B_2^T \left(A_{22}^{-1}\right)^T q_p^T q_p A_{22}^{-1} B_2.$$

Note that in the present case $B_2 = 0$. However, this matrix is included above to demonstrate that in the more general case we may have nonzero N_0 in the perturbed cost functional.

The convergence of the perturbation method is shown in Table 4.3.3. The deviation at $\varepsilon = -1 \times 10^{-7}$ indicates that $|\varepsilon|$ should not be made smaller than 10^{-6} in this case.

The next question is whether the converged solution to the perturbed system P_0 also satisfies eq. (4.60). Table 4.3.3 indicates that this is not the case. Hence, the perturbation

ε	Index of P_0					
	$(1,1)$	$(1,2)$	$(1,3)$	$(1,4)$	$(1,5)$	$(1,6)$
-1E-4	-8.185E-11	6.732E-10	2.085E-10	1.320E-9	8.497E-10	1.383E-9
-1E-5	-8.427E-11	6.778E-10	2.063E-10	1.327E-9	8.496E-10	1.390E-9
-1E-6	-8.444E-11	6.778E-10	2.045E-10	1.326E-9	8.478E-10	1.387E-9
-1E-7	-2.800E-11	5.493E-10	1.641E-10	1.433E-9	1.027E-9	1.624E-9

Table 4.5: Some elements of P_0 for the rotating cylinder control problem for several values of ε with 130 control volumes and $Q_p \neq 0$.

Norm	$P = P_0^{\#}$	$P = P_\infty^{\#}$
$\|\cdot\|_1$	1.20E-2	2.19E-2
$\|\cdot\|_2$	1.03E-2	1.02E-2
$\|\cdot\|_\infty$	3.73E-2	4.57E-2
Frobenius	1.05E-2	1.14E-2

Table 4.6: Residuals for eq. (4.60) for the rotating cylinder control problem with $\varepsilon = -1 \times 10^{-6}$, $Q_p \neq 0$, and 130 control volumes.

method is invalid for $Q_p \neq 0$.

4.3.4 Numerical Solution to the Riccati Equation

The *lqr* algorithm in Matlab has not been designed for large sparse systems. As a result, some numerical difficulties are encountered when the system becomes large, as is evidenced by Table 4.2. Alternative numerical algorithms have been developed for large sparse systems, especially using Chandrasekhar methods (Borggaard et al, 2004; Banks and Ito, 1991).

4.3.5 Further Numerical Considerations

The numerical results of this section were produced using the Stokes linearization (eq. (4.75)), which is a linearization of the Navier-Stokes equations about the origin. Defining the Reynolds' number of the system:

$$Re = \frac{\rho \bar{\mathbf{V}} l}{\mu} \tag{4.78}$$

with l the width of the channel and $\bar{\mathbf{V}}$ the inlet velocity, it is clear that when the Reynolds number is small the nonlinear term in eqs. (4.1)-(4.2) will also be small and the flow will ressemble Stokes flow. Hence, this linearization can be regarded as fairly accurate for low Reynolds' number flow. However, when the Reynolds' number is large the nonlinear term becomes much more significant and the Stokes linearization will no longer be appropriate. Instead, the Oseen linearization (eq. (4.76)) will be more appropriate. However, this introduces some inhomogeneity into the state equations which does not comform with the form of eqs. (4.59) and (4.60).

4.4 Simulation

The trajectory of the control problem was also analyzed under several conditions.

4.4.1 Numerical Results for Optimal Drag Reduction by the Stokes Method

The problem was simulated on a mesh of 132 nodes with a Reynolds number of 2000. The inlet velocity is constant at 1m/s and the channel is 5m long and has a 2m span. The value of R was kept small at $R = 10^{-7}$. The problem was then simulated over 10s with 1000 time steps. Figure 4.2 shows the final flow field though it is rather uninformative as to the performance of the control.

To investigate the effectiveness of the control we can calculate the performance index J at each time step to directly track performance. The increase in J at a particular time step is given by

$$\begin{aligned} \Delta J &= L(t)\Delta t, \\ L(t) &= \mathbf{x}^T Q \mathbf{x} + \mathbf{u}^T R \mathbf{u}. \end{aligned} \tag{4.79}$$

This information is plotted in Figure 4.3. Since the control law is an infinite-horizon optimal control, it is expected that a minimum should be produced at steady state. But, Figure 4.3 suggests that a minimum is not attained at steady state. However, noting that the control takes on very small magnitudes, this may or may not be attributed to some small numerical error. To determine the steady state optimal control the integrand of the cost

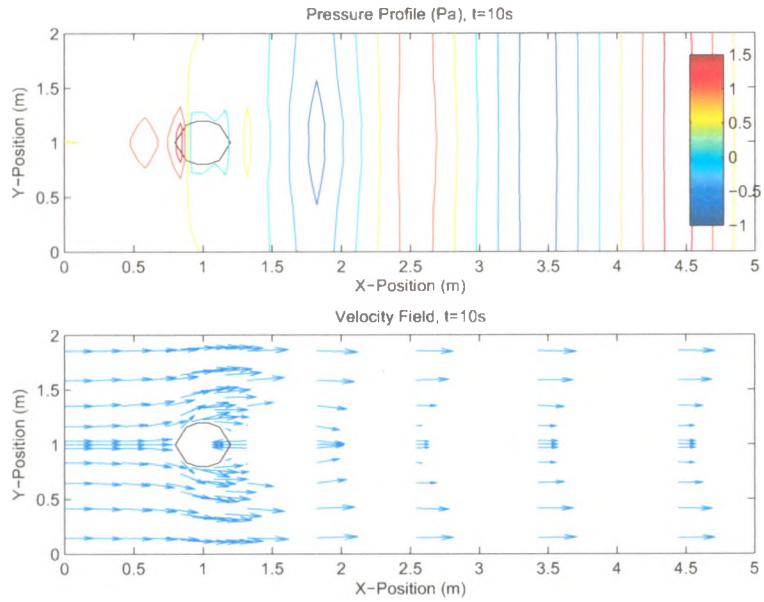

Figure 4.2: Final flow field for the skin friction reduction problem with $R = 10^{-7}$, $\mathrm{Re} = 2000$, and 132 control volumes.

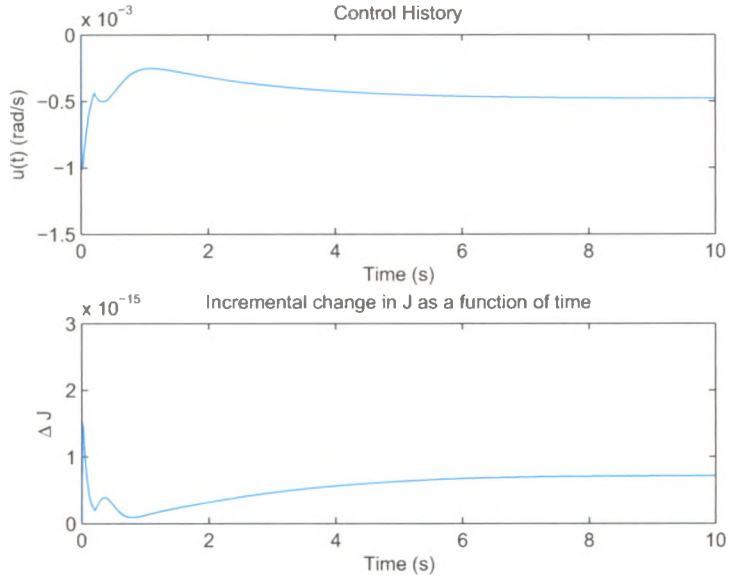

Figure 4.3: Control and cost functional history for the drag control problem with $R = 10^{-7}$, $\mathrm{Re} = 2000$, and 132 control volumes.

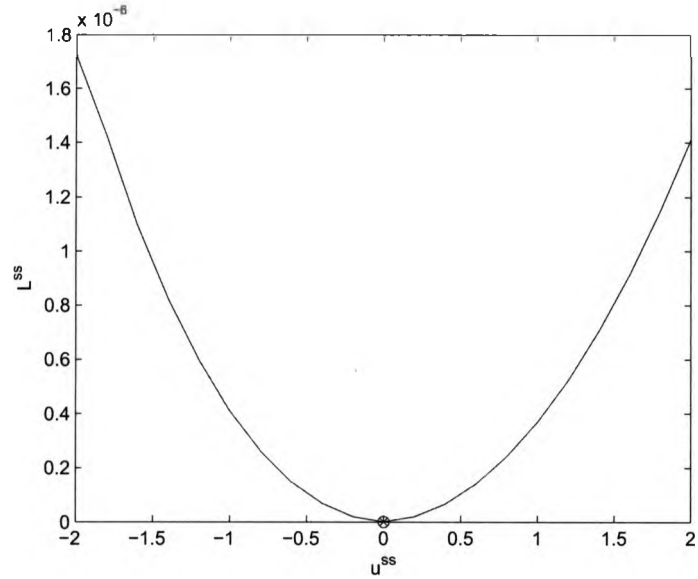

Figure 4.4: Steady state evaluation of L for $R = 10^{-7}$, $\mathrm{Re} = 2000$, and 132 control volumes for the drag minimization problem. The steady state solution to the optimal control problem is marked by $\otimes$.

functional at steady state L^{ss} can be plotted for a range of steady state values of u^{ss}. This information is displayed in Figure 4.4, from which the steady state solution can be read as $u^{ss} = 0$.

4.4.2 Numerical Results for Specific Velocity Control by the Stokes Method

The fact that the minimum occurs at $u^{ss} = 0$ indicates that this control problem is not suitable to evaluate the validity of the control law. Therefore, a second control problem is proposed whereby the control law should minimize the velocity at a point slightly north of the cylinder at position $(\xi, \eta) = (1, 1.32)$. Intuitively, if the cylinder is rotating counter-clockwise it should induce the effect of slowing the flow rate above the cylinder and hence the solution is expected to have a non-zero steady state solution. The control problem was solved over 132 control volumes with 1000 times steps, $R = 10^{-3}$, and $\mathrm{Re} = 2000$. The control history is displayed in Figure 4.5. Figure 4.6 indicates that there is a significant discrepancy between the steady state optimal control and the steady state control produced

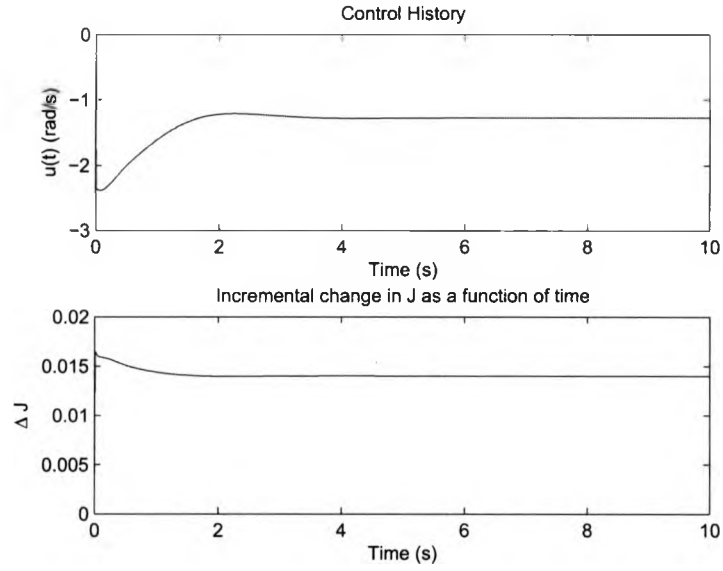

Figure 4.5: Control history for the specific velocity control problem with $R = 10^{-3}$, $\mathrm{Re} = 2000$, and 132 control volumes.

by this linearization.

The inaccuracy of the feedback law evident in Figure 4.6 may be due to the use of the Stokes linearization. Reducing the density will result in a flow field more characteristic of Stokes flow. In particular, the density of the fluid should be low. For this simulation, we use $\rho = 0.001\mathrm{kg/m}^3$ and $\mu = 0.001Ns/m$, resulting in $\mathrm{Re} = 2$. The control history is shown in Figure 4.7 and the steady state control law is shown in Figure 4.8. Once again, a steady state minimum has not been produced.

4.4.3 Advantages of the Oseen Linearization

Control of nonlinear systems by a linear control law is well-established. Generally in such cases the system is linearized about the equilibrium point before applying the control. In this way, the linearized system dynamics will approach the dynamics of the nonlinear system as the system approaches equilibrium and hence if $J = \frac{1}{2}\int_0^\infty L(t)\,\mathrm{dt}$ then the equilibrium point should be a minimum for $L(t)$. In the case of the Stokes problem, the linearization point is the origin, which is far from the equilibrium point. It is therefore expected that the equilibrium point obtained from the Stokes problem should not coincide with the

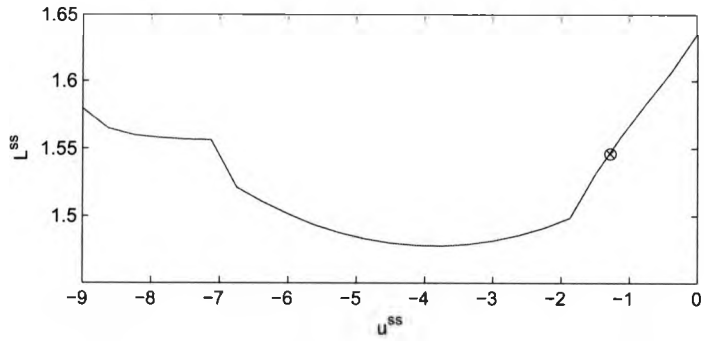

Figure 4.6: Steady state evaluation of L for $R = 10^{-3}$, Re $= 2000$, and 132 control volumes for the specific velocity control problem. The steady state solution to the optimal control problem is marked by $\otimes$.

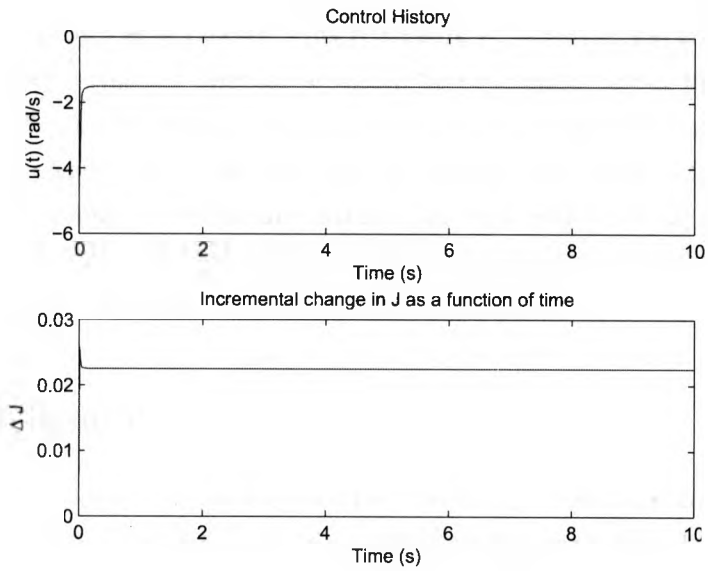

Figure 4.7: Control history for the specific velocity control problem with $R = 10^{-3}$, Re $=$ 2, and 132 control volumes.

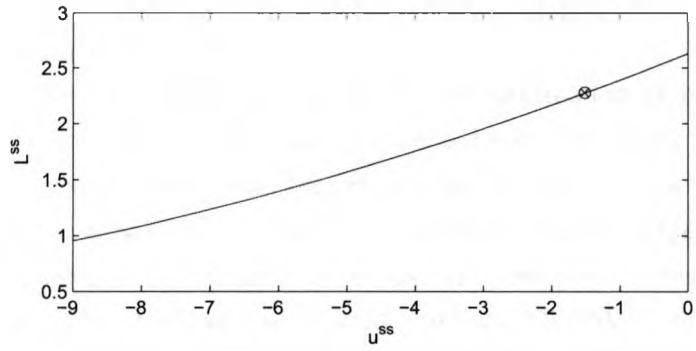

Figure 4.8: Steady state evaluation of L for $R = 10^{-3}$, Re $= 2$, and 132 control volumes for the specific velocity control problem. The steady state solution to the optimal control problem is marked by $\otimes$.

minimum steady state solution, which is certainly the case in this example.

To obtain better results, the system could be linearized about the current state (Oseen problem) at each time step and the feedback law could be generated based on this linearization. If the control law is solvable and the system generated by this procedure converges then the equilibrium point reached should indeed be a minimum. This procedure has been demonstrated in Brown et al (2009). This procedure is, however, too computationally expensive in practice. Another alternative would be to linearize about the initial state and develop the feedback law for this Oseen problem. This will again not converge to the actual minimum at steady state but would certainly produce better results than those obtained from the Stokes problem since the linearization point would be closer to the actual state of the system. The difficulty in applying this method to the Navier-Stokes equations is the introduction of an inhomogeneous term into the state equation.

4.5 Conclusions

This paper has addressed the problem of linear quadratic feedback control of the finite volume discretized Navier-Stokes equations. Riccati equations were developed under the conditions $B_2 = 0$, $C_1 = 0$, $C_2 = 0$. The perturbation method was investigated as a viable solution alternative to direct numerical solution of the system Riccati equations by substituting the perturbed solution into the Riccati equations. The results showed that when $Q_p = 0$ the solution to the perturbed system was also a solution to the second Riccati equation (4.60) and possibly also a solution to the first Riccati equation (4.59) though the results

could not be interpreted conclusively. The solution to the perturbed system did not satisfy the second Riccati equation (4.60) when $Q_p \neq 0$.

Though the numerical analysis did indicate that the perturbation method may have generated the optimal solution, the simulation results did not support this theory. However, there are several possible reasons why the perturbation method may not have converged to the desired result, the most likely of which is the treatment of the Dirichlet boundary condition in the Stokes method. Though the inlet conditions correspond to the velocity variable, they are treated as constant and so it seems that setting the Dirichlet boundary condition to 0 may have been erroneous, regardless of the linearization point. If the non-zero Dirichlet boundary condition must be included in the Stokes linearization then this method is redundant, and the Oseen linearization should be used instead. A change of variable can then be used to transform the system into a homogeneous one. This is recommended for future work.

References

Banks HT, Ito K (1991) A numerical algorithm for feedback gains in high dimensional lqr problems. SIAM Journal of Control and Optimization 29:499–515

Borggaard J, Burns J, Zietsman L (2004) Computational challenges in control of partial differential equations. In: 2nd AIAA Flow Control Conference

Brocket RW (1969) Finite Dimensional Linear Systems. John Wiley & Sons, Inc.

Brown D, Zhang C, Jiang J (2009) Feedback control of heat transfer systems by the numerical method of lines. In: The 2009 ASME Summer Heat Transfer Conference

Bryson AE, Ho YC (1969) Applied Optimal Control. Blaisdell Publishing Company

Drazin PG (2002) Introduction to Hydrodynamic Stability. Cambridge University Press

Gad-el-Hak M, Bewley TR (2006) MEMS: Introduction and Fundamentals, CRC Press, chap 15

Högberg M, Bewley TR, Henningson DS (2003) Linear feedback control and estimation of transition in plane flow. Journal of Fluid Mechanics 481:149–175

Liseikin VV (1999) Grid Generation Methods. Springer

Pinch ER (1993) Optimal Control and the Calculus of Variations. Oxford University Press Inc.

Stoyanov MK (2006) Optimal linear feedback controller for incompressible fluid flow. Master's thesis, Virginia Polytechnic Institute and State University

Thompson JF, Warsi ZUA, Mastin CW (1985) Numerical Grid Generation: Foundation and Applications. Elsevier Science Publishing Co., Inc.

Chapter 5

Conclusions and Future Work

This thesis has addressed the problem of performance optimization for time-varying systems of multiple parameter types using two approaches. In the first approach, the discrete adjoint method has been developed for the purpose of performance optimization of fluid flow or heat transfer systems with respect to a combination of geometric and control variables. The method was successfully applied to a simple two dimensional fluid flow system. The simulation emphasized certain computational limitations of the method, especially data storage for the transient case. The simulation also indicated that some insight into the design problem can be beneficial, since the number of iterative steps required by the algorithm to reach the optimum can depend significantly on the starting point. Running the optimization algorithm over the individual parameter types first can be useful in determining a suitable starting point for the coupled optimization algorithm. Overall, the discrete adjoint method employed to calculate the gradient provides a significant improvement to computational time than using a finite difference approximation to the gradient. The only disadvantage is that the programming details are somewhat more challenging, and it is especially important to note that the details will depend on the way the problem is descretized and the way the control problem is parameterized. These problems can both be addressed by integrating the optimization algorithm into commercial software.

The second subject analyzed in this thesis was the application of a feedback control law to the Navier-Stokes equations. The proposed application method was to discretize the Navier-Stokes equations spatially and apply the feedback law to the partially discretized continuous-time equations. To investigate whether this method could in fact produce reasonable results, the control method was applied directly to

a simple one-dimensional heat transfer system. The numerical simulations indicated that the method was valid and that good results could be obtained by using a mobile linearization point.

Many inherent challenges exist in the application of feedback laws to the Navier-Stokes equations, particularly due to the degenerate form of the discretized equations and also the large number of equations generated by their full or partial discretization that are needed to obtain accurate numerical solutions. This problem was approached directly from first principles assuming the finite-volume discretization and formulated as a linear quadratic regulator problem. The control feedback problem was transformed into a nonlinear algebraic Riccati-form system, which we could not solve either analytically or numerically. However, we were able to use a perturbation method to obtain a solution matrix to this Riccati system numerically and use some numerical analysis to assess the validity. Though not entirely conclusive, the numerical results indicated some promising results under certain limiting conditions.

Though the numerical investigation was not entirely conclusive, the system performance associated with the feedback law was evaluated to determine whether the control law was valid. A comparison was made between the steady state solution obtained from the feedback law and the performance at steady state for a range of control inputs. This comparison indicated that the feedback law had not functioned as indended.

Though the final result of the feedback control problem did not indicate success, the exact cause of this is unclear. The perturbation method appears to be valid though a more rigorous analysis of this method may determine this more conclusively. There is also the possibility of a simple coding error, thought much time has been dedicated to testing and validating the codes numerically. Most likely, the error is in the linearization process. The system was linearized about the origin to remove the Dirichlet boundary condition from the equations to produce a homogeneous system. However, we may consider that the Dirichlet boundary condition itself is treated as a

constant at steady state even in its partially discretized form, and so this linearization may have been performed incorrectly. Since the inclusion of the Dirichlet boundary condition seems unavoidalbe, the system will unavoidably be inhomogeneous, and so we may as well use the Oseen lienarization. In future work, the method can be modified to be linearized about the initial state rather than the origin using the Oseen linearization and a change of coordinates to the velocity variable at the boundary to maintain a homogeneous form of the equations. Since the variable being linearized appears in nonlinear terms, this may provide further challenges which have yet to be addressed.